Hindawi
Geofluids
Volume 2021, Article ID 8844312, 21 pages
https://doi.org/10.1155/2021/8844312

Research Article

Constraints of S–Pb–Sr Isotope Compositions and Rb–Sr Isotopic Age on the Origin of the Laoyingqing Noncarbonate-Hosted Pb–Zn Deposit in the Kunyang Group, SW China

Hongsheng Gong,[1,2] **Runsheng Han**,[1,2] **Peng Wu**,[1,2] **Gang Chen**,[1] **and Lingjie Li**[2]

[1]*Kunming University of Science and Technology, Faculty of Land Resources Engineering, Kunming, 650093 Yunnan, China*
[2]*Kunming University of Science and Technology, Southwest Institute of Geological Survey, Geological Survey Center for Non-ferrous Metals Resources, Kunming, 650093 Yunnan, China*

Correspondence should be addressed to Runsheng Han; 554670042@qq.com

Received 23 October 2020; Revised 14 January 2021; Accepted 25 January 2021; Published 8 February 2021

Academic Editor: Henrik Drake

The Laoyingqing Pb–Zn deposit is located on the southwestern margin of the Yangtze block and on the east side of the Xiaojiang deep fault in the Sichuan–Yunnan–Guizhou Pb–Zn metallogenic triangle area (SYGT). This deposit was first discovered in the silty and carbonaceous slate of the Middle Proterozoic Kunyang Group that is structurally controlled by thrust faults and anticlines. This study is aimed at investigating whether the Laoyingqing deposit has the same ore-forming age and type as other Pb–Zn deposits related to the Pb–Zn metallogenic system and prospecting prediction of the deep and peripheral areas of the deposits in the SYGT. Based on the sphalerite Rb–Sr age dating and S–Sr–Pb isotopic composition analysis of the Laoyingqing Pb–Zn deposit, the following results were obtained. First, the Rb–Sr isochron age of sphalerite is 209.8 ± 5.2 million years (Ma), consistent with the ages of most Pb–Zn deposits in the SYGT (approximately 200Ma), thereby potentially indicating that these Pb–Zn deposits may have been formed synchronously during the late Indosinian orogeny. Second, the Pb isotopic compositions of sulfides show a linear trend on the average crustal Pb evolution curve in $^{207}Pb/^{204}Pb$ vs. $^{206}Pb/^{204}Pb$ plot. In addition, Pb isotopic ratios were consistent with the age-corrected Pb isotopic ratios of basement rocks, consequently suggesting that the source of mixed crustal Pb is mainly derived from basement rocks. Combined with the initial $^{87}Sr/^{86}Sr$ ratios of sphalerite between the $(^{87}Sr/^{86}Sr)_{200Ma}$ value of the basement rocks and that of the Upper Sinian–Permian carbonates, it can be concluded that the ore-forming metals were mainly derived from basement rocks. Third, sulfur isotopic composition of sphalerite from the Laoyingqing deposits shows $\delta^{34}S_{CDT}$ values that range mainly from -2.62‰ to 1.42‰, which is evidently lower than the $\delta^{34}S_{CDT}$ values of sulfides (8–20‰) from other Pb–Zn deposits in the SYGT. This can be interpreted as a result of mixing with reduced S that was mainly derived from the thermochemically reduced S in the overlying strata and a small amount of reduced S produced by the pyrolysis of S-containing organic matter. We conclude that the Laoyingqing deposit and most of the Pb–Zn deposits in the SYGT are Mississippi Valley-type deposits, thereby providing new ideas for investigating the deep and peripheral areas of Pb–Zn deposits.

1. Introduction

The contiguous Sichuan–Yunnan–Guizhou Pb–Zn metallogenic triangle area (SYGT) (Figure 1(a)), located in the southwestern margin of the Yangtze Block in China, is an important part of the South China low-temperature metallogenic domain [1–4]. There are more than 440 carbonate-hosted Pb–Zn deposits distributed in the SYGT and the metal resources exceed 26 million tons, which makes SYGT the largest Pb–Zn mining area and the area with the highest metallogenic potential in China [5]. These Pb–Zn deposits have high grades of Pb+Zn (generally >15%) and are rich in various elements, such as Cd, Ga, Ge, and Ag [6–8]. The deposit concentration district in Northeast Yunnan is confined by the NS-trending Xiaojiang Fault zone, NE-trending Mile–Shizong Fault zone, and NW-trending Ziyun–Yadu Fault zone. The area's strong multistage structure superposition, variable geological environment with complex

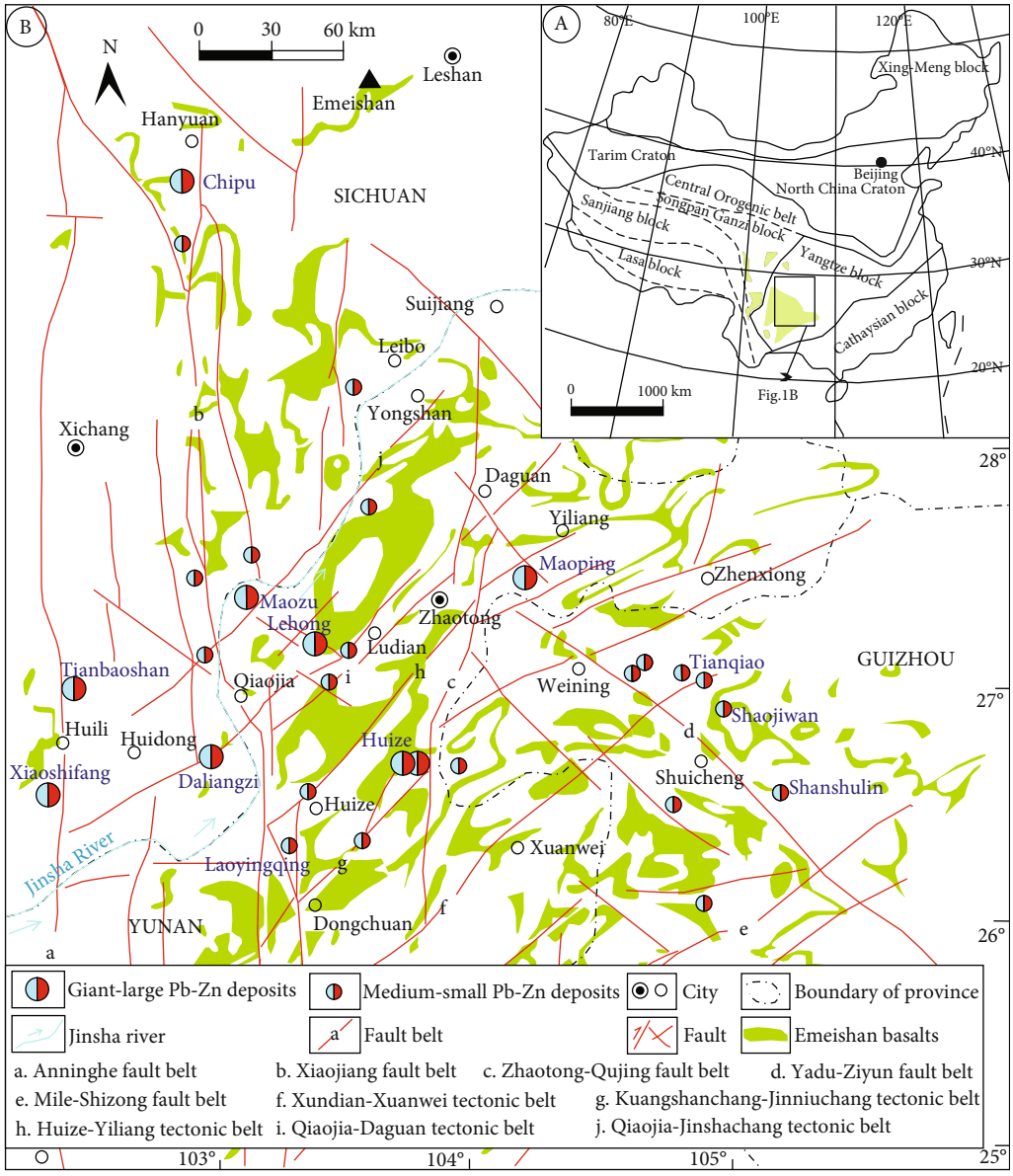

Figure 1: Regional geological map. Panel A: simplified tectonic map of South China (after [7, 31]). Panel B: regional geological map of the SYGT, SW China, showing the spatial relationships among the fault belts, Emeishan basalts, and major Pb–Zn deposits (modified from [6]).

metallogenic dynamic mechanisms, and superior metallogenic conditions formed the unique Ge-rich Pb–Zn polymetallic deposit concentration district and created a massive world-class deposit (Huize Pb–Zn deposit, with a Pb–Zn reserve of 7 million tons) of a rare super-high grade (Pb+Zn: 25–35%) (Figure 1(b)). The area is typical in the SYGT [9], and it has become a hot spot for ore deposit studies.

In addition to the Huize Pb–Zn deposit, there are six additional large Pb–Zn deposits in the SYGT, which are referred to as Maoping [10, 11], Maozu [12], Lehong [13, 14], Daliangzi [13, 15], Tianbaoshan ([16, 17]), and Chipu ([13, 18]; Table 1). Previous studies have proposed different models of the genesis of the SYGT Pb–Zn deposits, and the main theories have posited a Mississippi Valley-type (MVT) genesis and a sedimentary dominated strata-bound genesis [6, 19–24]. Recent studies have suggested that most of the Pb–Zn ore bodies in the SYGT are hosted in the Upper Sinian to Lower Permian carbonate rocks [6, 9, 13, 25] and that these deposits formed during the late Indosinian orogeny (approximately 200 Ma, Table 1). Furthermore, the $\delta^{34}S$ value of these deposits is generally in the range of 8‰ to 20‰, which indicates that the reduced S within these deposits was mainly derived by thermochemical sulfate reduction (TSR) of seawater sulfates available in the host rocks [2, 26–30].

The Kunyang or Huili Groups in the basement are generally considered as sources for ore-forming elements in the Pb–Zn deposits of the SYGT [24, 32, 33]. Currently, two Pb–Zn deposits hosted in the Mesoproterozoic strata have been found in the SYGT. One is the Xiaoshifang Pb–Zn deposit in Huili, whose ore body is hosted in the calcareous slate of the Huili Group from the Mesoproterozoic; this is a

Table 1: Comparison of the major Pb–Zn deposits in the SYGT with MVT worldwide.

Deposits	Province	Reserves and grade	Host rocks	Ore-controlling structures	Orebody	Ore-forming fluids	Alteration	Ore–forming age (Ma) and test method	References
Huize	NE Yunnan	>6Mt Pb+Zn; 900t Ge; >25% Pb+Zn	Early Carboniferous dolostone	NE-trending thrust faults	Stratiform, lenticular	Salinity: 6–12 wt.% NaCl; Th: 164–220°C	Dolomitisation, calcification, silification,	223.5 ± 3.9, 226 ± 6.4, 196.3 ± 1.8 (sphalerite Rb–Sr)	Han et al. [52], Yin et al. [53]
Maoping		>3Mt Pb+Zn; >25% Pb+Zn	Late Devonian and Carboniferous dolostone and limestone	NW-trending faults and anticline	Stratiform, lenticular, vein	Salinity: 6.7–13.8 wt.% NaCl; Th: 123–206°C	Dolomitisation, calcification, silification	No data	Han et al. [10], Wang et al. [11]
Maozu		>1Mt Pb+Zn; >12% Pb+Zn	Late Sinian dolostone	NE-trending thrust -fold	Stratiform	Salinity: 2.8–5.3 wt.% NaCl; Th: 153–248°C	Silification, baritization, fluoritization	196 ± 13 (calcite Sm–Nd)	Zhou et al. [12]
Lehong		6–12% Pb+Zn	Late Sinian dolostone	NW-trending fault	Stratiform, lenticular, vein	Salinity: 11.3–14.5 wt.% NaCl; Th: 165–229°C	Baritization, dolomitisation, ferritization	200.9 ± 8.3 (sphalerite Rb–Sr)	Zhang et al. [14], Wu [13]
Laoyingqing		<0.1Mt Zn; <10% Zn	Mesoproterozoic Kunyang Group silty and carbonaceous slate	NE-trending thrust faults, NW-trending thrust faults, and anticline	Vein	Salinity: 7.17–20.67 wt.% NaCl; Th: 130–275°C	Silicification, carbonatisation	209.8 ± 5.2 (sphalerite Rb–Sr)	This paper
Daliangzi		>1Mt Pb+Zn; >10% Pb+Zn	Late Sinian dolostone	NW-trending thrust faults	Lenticular, vein, cystic	Salinity: 18 wt.% NaCl; Th: 170–225°C	Carbonatisation, silification, dolomitisation	204.4 ± 1.2 (calcite Sm–Nd)	Wu [13], Zhang et al. [15]
Tianbaoshan	SW Sichuan	2.6Mt Pb+Zn; 6–12% Pb+Zn	Late Sinian dolostone	NW-trending thrust faults	Stratiform, lenticular, vein	Salinity: 12.4–20 wt.% NaCl; Th: 157–267°C	Dolomitisation, calcification, silification	>166 (zircon U–Pb age of diabase)	Wang et al. [16], Zhou et al. [17]
Chipu		>12% Pb+Zn	Late Sinian dolostone	NW-trending thrust faults	Stratiform, lenticular	Salinity: 8.5–17 wt.% NaCl; Th: 130–250°C	Silification, calcification, bituminization	292.0 ± 9.7, 165.7 ± 9.9 (bitumen Re–Os)	Wu [13], Wu et al. [18]
Shanshulin	NW Guizhou	>0.5Mt Pb+Zn; >20% Pb+Zn	Late Carboniferous dolomitic limestone	NW-trending thrust faults	Stratiform, vein	Salinity: < 15 wt.% NaCl; Th: 150–280°C	Calcification, dolomitisation	No data	Zhou et al. [54]
Shaojiwan					Stratiform			No data	

Table 1: Continued.

Deposits	Province	Reserves and grade	Host rocks	Ore-controlling structures	Orebody	Ore-forming fluids	Alteration	Ore–forming age (Ma) and test method	References
		>0.4Mt Pb+Zn; >12% Pb+Zn	Early Permian and middle Devonian dolomitic limestone and dolostone	NW-trending thrust-fold		Salinity: 0.9–17.5 wt.% NaCl; Th: 115–170°C	Calcification, dolomitisation		Zhou et al. [55]
Tianqiao		>0.3Mt Pb+Zn; >15% Pb+Zn	Carboniferous dolostone	NW-trending thrust-fold	Stratiform	Salinity: 9.6–14.2 wt.% NaCl; Th: 150–270°C	Calcification, dolomitisation	191.9 ± 6.9 (sphalerite Rb–Sr)	Zhou et al. [8]
MVT	Worldwide	Generally, medium-small scale for single deposits but can be large in an ore district	Platform carbonate (mainly dolostone)	Fault and fractures, collapsed breccia, phase transition, basement uplift, bioherm	Stratiform vein	Th: 75–200°C	Calcification, wall rock dissolution, organics, silicification	Main formation ages: Devonian to Triassic, Cretaceous to Paleogene	Leach and Sangster [56], Leach et al. [57]

volcanic-hosted massive sulfide (VHMS) type Pb–Zn deposit formed in the Early Cambrian [34, 35]. The other example is the Laoyingqing Pb–Zn deposit located in the deposit concentration district in Northeast Yunnan. The ore body is hosted in the fracture zone of the silty and carbonaceous slate of the Kunyang Group from the Mesoproterozoic. The Laoyingqing Pb–Zn deposit is unique within the SYGT and evidently different from the Xiaoshifang Pb–Zn deposit. Determining whether the Laoyingqing deposit has the same ore-forming age and type as those of other Pb–Zn deposits is directly related to understanding the Pb–Zn metallogenic system of the region and can benefit the prospecting prediction of the deep and peripheral areas of the deposits in the SYGT. However, there are few previous studies on the ore-forming age, material source, and genesis of the Laoyingqing Pb–Zn deposit.

Isotopic geochemistry is a powerful tool for studying hydrothermal deposits. Direct dating of hydrothermal deposits is key for the correct evaluation of their relationships with geotectonic events. However, due to the lack of suitable minerals for traditional radioisotope dating, this process is more difficult [36–38]. In recent decades, the sphalerite Rb–Sr age dating method has been greatly improved and has become an ideal tool for the direct dating of minerals in Pb–Zn deposits [37, 39–43]. However, the reliability of the sphalerite Rb–Sr dating method has been questioned due to the possibility of contamination with carbonate, clay, or volcanic ash inclusions resulting in erroneous $^{87}Sr/^{86}Sr$ ratios ([44, 45]). It has been experimentally demonstrated that the Rb–Sr isotopic compositions of residual solid samples after crushing and cleaning can be used to date a deposit [46]. The Rb–Sr isochron ages obtained by this method in the MVT deposits of the Polaris and upper Mississippi Valley areas are the same as their paleomagnetic ages; therefore, these ages were considered to represent the mineralisation ages [46]. At present, in terms of constraining the geodynamic settings of carbonate-hosted Pb–Zn deposits, the sphalerite Rb–Sr geochronology has been widely used (e.g., [47–51]). For instance, it has been recently reported that high-spatial in-situ Rb–Sr dating of fine-grained mineral slickenfibres within faults can constrain the time of fault activity and resolve the complex histories of fault reactivation[58]. The stable isotopes of S, Pb, and Sr are powerful tools that can be used to constrain the source of ore-forming metals and fluids, as well as fluid migration pathways (e.g., [57, 59–62]). However, there are few studies on these isotopic systems in the Laoyingqing Pb–Zn deposit.

In this study, we performed a comparative analysis of the Laoyingqing Pb–Zn deposit and other relevant Pb–Zn deposits in the SYGT, in terms of ore deposit geology, ore-forming ages, and ore-forming material sources, so as to determine the genesis of the Laoyingqing Pb–Zn deposit and the relationship with other deposits in the SYGT. The comparison is based on sphalerite Rb–Sr isochron age dating and systematics of S–Pb–Sr stable isotopes which helped reveal the metallogenic dynamic background and the differences in the source of ore-forming materials of different deposits in the SYGT. The results provide new insights into the genesis of the Laoyingqing Pb–Zn deposit, a reference for the study of Pb–Zn metallogenic systems in the SYGT, and provide new ideas for investigating the deep and peripheral areas of Pb–Zn deposits in the SYGT.

2. Regional Geology

The SYGT is located in the southwestern margin of the Yangtze block (Figure 1(a)), which is a triangular area bounded by the SN-trending Anninghe Fault, the NW-trending Yadu–Ziyun Fault, and the NE-trending Mile–Shizong Fault. There are many SN faults matched with NE and NW secondary faults and folds in the area [63]. Five thrust-fold belts controlled by NE structures have developed in the deposit concentration district in Northeast Yunnan, namely, Xundian–Xuanwei, Kuangshanchang–Jinniuchang, Huize–Yiliang, Qiaojia–Daguan, and Qiaojia–Jinshachang structural belts. These belts are distributed in a "multi-character" pattern, which is typical of the wide-scale patterns in Northeast Yunnan [10, 64, 65] (Figure 1(b)).

The regional strata are mainly composed of basement and sedimentary covers. The basement is mainly composed of the Archaeozoic–Palaeoproterozoic crystalline basement and the Mesoproterozoic folded basement [6]. Exposures of this region include the folded basement of the Dongchuan and Kunyang Groups (Huili Group) which are a set of shallow marine flysch clastic rocks intercalated with volcanic rocks mainly composed of graywackes, slates, and other carbonaceous to siliceous sedimentary rocks [66, 67]. Thick marine sedimentary rocks were deposited from Neoproterozoic to the early Mesozoic. Among them, Sinian rocks mainly consist of thick dolomite; Cambrian deposits are characterised by shale and sandstone; Ordovician to Silurian strata are mainly composed of carbonate, argillaceous siltstone, and shale; Devonian sediments mainly comprise sandstone, siltstone, and carbonate; Carboniferous to Permian strata are mainly composed of carbonate and basalt; Triassic sediments mainly comprise sandstone, mudstone, and partly carbonate rock. During the Middle-Late Triassic, a strong oblique thrust-slip was induced in the foreland basin due to the closure of the Paleo-Tethys Ocean and orogenic events in the region (Indosinian orogeny, 250–230 Ma; [68, 69]), which resulted in the formation of a series of thrust-fold structures (zones) [70–72].

The SYGT Pb–Zn deposits are mainly controlled by thrust faults. The ore bodies occur in the carbonate rocks from Neoproterozoic to Permian and occur in stratiform lenticular and veined forms (Table 1). Metallic minerals that occur in the deposits are mainly sphalerite, galena, and pyrite, whereas the nonmetallic minerals are mainly calcite, dolomite, and quartz. The wall rock alterations of the SYGT deposit are mainly dolomitisation, calcitisation, and silicification. The structural system in the region is very complex, which controls the distribution of the Pb–Zn deposits. The NS-trending faults in the west of the SYGT controlled the distribution of the Daliangzi, Tianbaoshan, Maozu, and Chipu deposits. The Tianqiao, Shaojiwan, and Shanshulin deposits in the east are distributed along the NW-trending Ziyun–Yadu Fault. The larger-sized deposits are usually distributed near the regional deep faults and the intersection of

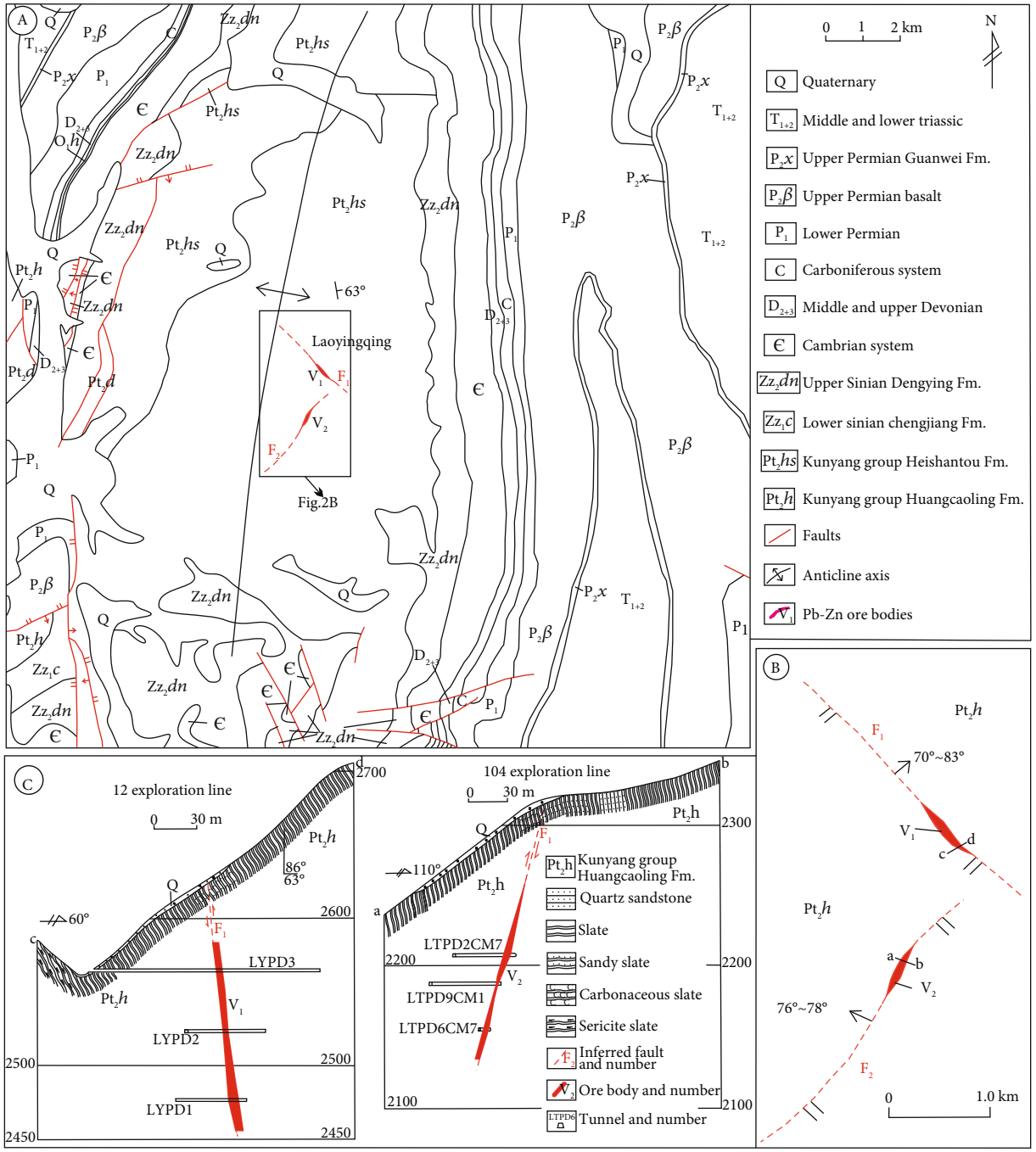

FIGURE 2: Geological map of the Laoyingqing Pb–Zn deposit. (a) Geological map of mining area. (b) Simplified geological map of the deposit. (c) Geological section of exploration line 12 of Laoyingqing ore block and Geological section of exploration line 104 of Laolongtian ore block.

faults. The Laoyingqing Pb–Zn deposit is located at the intersection of the SN-trending Xiaojiang fault and the NE-trending Dongchuan–Huize–Zhenxiong Fault (Figure 1(b)).

3. Geology of the Laoyingqing Deposit

The Laoyingqing Pb–Zn deposit is located towards the east of the Xiaojiang Fault and in the core of the Wuxing anticline located in the western portion of the NNE-trending Dongchuan–Wuxing–Luozehe structural belt. The strata cropping out in the Laoyingqing ore-field include the Huangcaoling (Pt_2h) and Heishantou Formations (Pt_2hs) of the Mesoproterozoic Kunyang Group, as well as the Sinian Dengying Formation (Zz_2dn) and Quaternary deposits (Q). The faults and folds in the ore-field mainly include NE-trending and NW-trending secondary faults and the SN-trending Wuxing anticline, which is a symmetrical anticline with a vertical axis and a strong secondary fold in its core. No magmatic rocks were exposed in the ore-field and surrounding areas. Under low-temperature dynamic metamorphism, the Huangcaoling (Pt_2h) and Heishantou (Pt_2hs) Formations of the Mesoproterozoic Kunyang Group in the ore-field formed a shallow

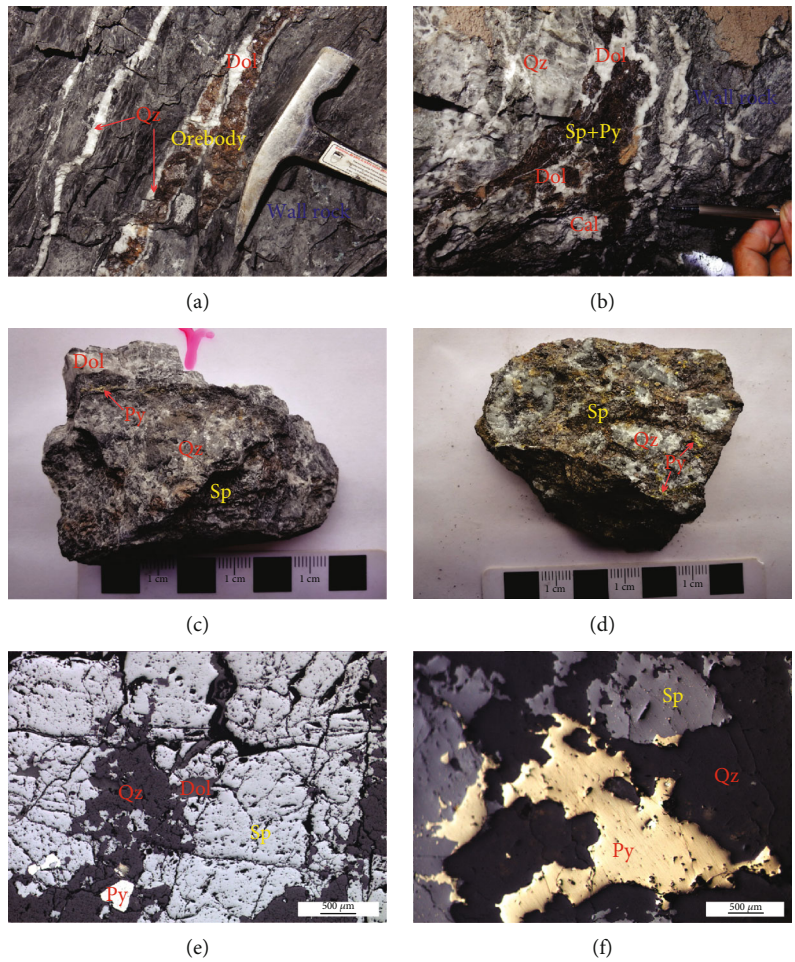

FIGURE 3: Field photos of ore bodies and wall rocks of the Laoyingqing Pb–Zn deposit. (a) The primary ore body in the silty and carbonaceous slate of the Huangcaoling Fm. in Mesoproterozoic Kunyang Group, and the distinctive boundary between the ore body and wall rocks. (b) The gangue quartz, calcites, and dolomites in primary ores. (c) Fine- to coarse-grained sphalerite (Sp)+lumpy and patch quartz (Qz)+vein pyrite (Py)+vein dolomite (Dol). (d) Fine-grained Sp+patch Qz+patch Py. (e) Coarse-grained Sp+cubic Py+vein Dol+quartz. (f) Fine-grained Sp+fine-grained Py+quartz. Abbreviations: Sp: sphalerite; Py: pyrite; Qz: quartz; Dol: dolomite; Cal: calcite.

metamorphic rock series such as slate and phyllite with metamorphic quartz sandstone and marble. The wall rock alterations that are mainly distributed in the fault fracture zone and the wall rocks near the ore body are strong and mainly demonstrate signs of silicification and carbonatisation (Figure 2(a)).

The V_1 and V_2 ore bodies in the Laoyingqing and Laolongtian sections, respectively, discovered in the Laoyingqing Pb–Zn deposit occur in the silty and carbonaceous slate of the Huangcaoling Formation (Pt_2h) and are, respectively, controlled by an NW-trending F_1 reverse fault and NE-trending F_2 reverse fault. The occurrence of the ore body is basically consistent with the fault. The F_1 fault has an inclination of 55°–65°, a dip angle of 70°–83°, and a fault fracture zone width of 1.6 m–16 m. The F_2 fault has an inclination of 292°–300°, a dip angle of 76°–78°, and a fault fracture zone width of 1.5 m–7.5 m. Both fracture zones are composed of zinc-bearing structural breccia and slate (fractured in F_1 and fragmented in F_2). The tunnels are used to control the blind ore bodies due to the steep occurrence of the two ore bodies (Figure 2(b)). The V_1 ore body has a length of 288 m, thickness of 3.56 m, and depth of 130 m. It contains 22764 tons of Zn metals and has a grade of 4.92 wt.% Zn. The V_2 ore body has a length of 250 m, a thickness of 3.10 m, a depth of 56 m, contains 10228 tons of Zn metals, and has a grade of 5.26 wt.% Zn (Figure 2(c)). The ore bodies have irregular vein shapes and are locally expanded and continuous. The ore metal minerals are mainly sphalerite, followed by a small amount of galena and pyrite; the ore gangue minerals are mainly quartz and calcite, followed by mica, dolomite, and chlorite. The ore contains inclusion structures and filling metasomatic structures; these structures are mainly breccia structures, followed by fine-grained star point structures, disseminated structures, fine vein-network structures, and massive structures (Figures 3(a) and 3(b)).

The ores of the Laoyingqing deposit have experienced syn-sedimentary, hydrothermal, and supergene processes. There are two main mineral assemblages formed during the hydrothermal period (Figure 4). In the sphalerite-pyrite-quartz assemblage formed in the early stage of mineralisation, the dark brown fine-grained sphalerite occurs in a lumpy and patchy form, the fine-grained pyrite is patchy in

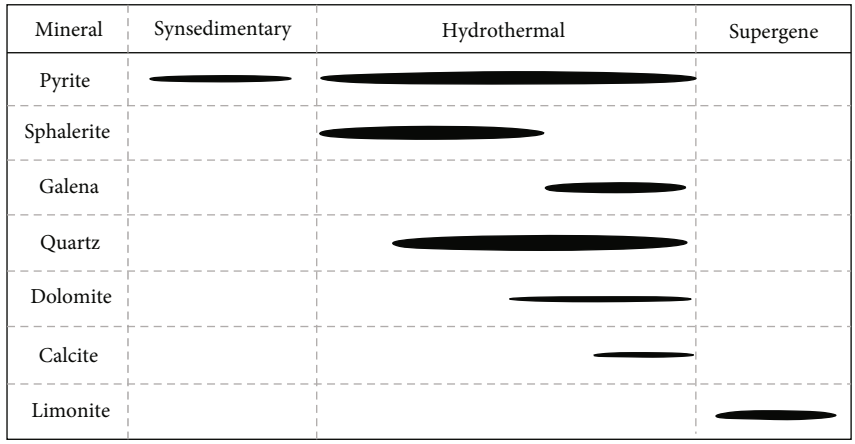

Figure 4: Mineral assemblages in the paragenetic sequence of the Laoyingqing Pb–Zn deposit.

the wall rocks around the ores, while quartz is both lumpy and patchy (Figures 3(d) and 3(f)). In the sphalerite-pyrite-quartz-dolomite assemblage of the middle-late stage mineralisation, the dark brown coarse-grained sphalerite occurs in a lumpy and patchy form, the coarse-grained pyrite in a cubic form as a fine vein, quartz in a lumpy and patchy form, and dolomite in the form of a vein (Figures 3(c) and 3(e)).

4. Samples and Analytical Methods

4.1. Sample Collection. In this study, eight representative primary metal sulfide ore samples from different middle sections of the V_1 and V_2 ore bodies were collected—six in V_1 and two in V_2. In each sample, sphalerite, galena, pyrite, quartz, calcite, and dolomite occurrence were observed, with seven samples of sphalerite, one sample of pyrite, and eight samples of quartz. Five sphalerites samples from V_1 were used for Rb–Sr radiogenic isotope analyses, and the seven sphalerites samples and one pyrite sample were used to analyse S and Pb stable isotopes. Seven ore samples were prepared by grinding them into double-sided polished fluid inclusion sheets (approximately 200 μm in thickness).

4.2. Analytical Methods. Microthermometry was performed at the fluid laboratory of the Southwest Institute of Geological Survey Centre for Non-ferrous Metal Resources. The instruments used included the Linkam THMS600 heating and freezing stage from the United Kingdom and a standard microscope equipped with an image analysis system. Prior to the experiment, the heating and freezing stages were calibrated with international synthetic fluid inclusion standard samples. When the temperature was lower than 0°C and higher than 200°C, the instrument error was ±0.1 and ±2°C, respectively.

The ore samples from the Laoyingqing Pb–Zn deposit were crushed to 40–60 mesh, and the minerals with high purity, as determined by microscope, were selected. These minerals were then ground to less than 200 mesh and sent to the laboratory for isotopic analyses.

For the Rb–Sr isotope analyses, the sample was washed with ultrapure water three times in an ultrasonic bath to remove the salts coming from broken fluid inclusions. An appropriate amount of mixed diluent of known concentration was added to the sample and dissolved with ultrapure 6 mol/L HCl and HNO_3 in a sealed Teflon cup. Then, the sample was heated in an oven at 200°C and evaporated until dry. Next, ultrapure 6 mol/L HNO_3 was used to redissolve the sample. These samples were then transferred to a cation exchange resin column to separate and purify Rb and Sr. For a detailed description of the experimental process, please refer to the description of Wang et al. [73, 74]. The isotopic ratios were measured on a Triton (00682t) Multicollector Thermal Ionization Mass Spectrometer (TIMS) at the Wuhan Geological Survey center, China Geological Survey. The instrument fractionation of the Sr isotope was corrected by analysing the international standard NBS-987. The measured standard value of $^{87}Sr/^{86}Sr$ was 0.710233 ± 6, which was consistent with the recommended value (0.71023 ± 5; [47]). The errors (2σ) of the $^{87}Rb/^{86}Sr$ and $^{87}Sr/^{86}Sr$ ratios were 2% and 0.02%, respectively. The Rb–Sr isochron age was calculated using the Isoplot/Ex version 3.22 software [75].

The S isotope analyses were performed at the Beijing Kehui Testing Technology Co. Ltd. using a 253 plus 10 kV Isotope Ratio Mass Spectrometer, a FlashSmart Elemental Analyzer, and a ConFlo IV multipurpose interface of Thermo Fisher Scientific of the United States. The sample was fully burned, and all the gases generated were fully oxidised through the redox reaction tube with the layered filling of WO_3 and Cu wires. Meanwhile, a small amount of generated SO_3 was reduced to SO_2 when passed through Cu wires. Subsequently, the SO_2 was separated from other impurity gases by a chromatographic column and supplied to the mass spectrometer for analysis. Three standard substances, IAEA-S3, GBW04414, and GBW04415, were used in the analysis, and the analysis accuracy of the standard samples was better than 0.2‰.

The Pb isotope analyses were conducted using the GV Isoprobe-T TIMS at Beijing Kehui Testing Technology Co. Ltd. The sample was first decomposed with HF+HNO_3 mixed acid, then evaporated to dryness after digestion. Concentrated nitric acid was added and evaporated to dryness

Table 2: Microthermometric data of the fluid inclusions from the Laoyingqing Pb–Zn deposit.

Hosted mineral	Generation	Quantity	Microthermometric data					Source
			*T*m-ice (°C)	*T*h (°C)		Salinity (wt.% NaCleqv)		
				Range	Mean	Range	Mean	
Sphalerites	Primary	13	-8.6– -17.6	132.5–216.5	174.4	12.39–20.67	17.14	This paper
Quartz	Primary	51	-4.5– -16.2	130.0–275.0	214.4	7.17–19.60	13.43	

Table 3: Sphalerite Rb–Sr isotopic compositions of the Laoyingqing Pb–Zn deposit.

Sample no.	Object	Rb/ppm	Sr/ppm	$^{87}Rb/^{86}Sr$	$^{87}Sr/^{86}Sr$	$(^{87}Sr/^{86}Sr)_{200Ma}$	Source
LYQ-2	Sphalerite	0.1335	0.1156	3.336	0.72829 ± 0.00006	0.7189	This paper
LYQ-3		0.04995	0.1193	1.208	0.72188 ± 0.00002	0.7185	
LYQ-6		0.03368	0.2523	0.3852	0.71950 ± 0.00003	0.7184	
LYQ-7		0.01197	0.09629	0.3589	0.72041 ± 0.00005	0.7194	
LYQ-8		0.0664	0.1369	1.401	0.72257 ± 0.00003	0.7186	

Note: $(^{87}Sr/^{86}Sr)_t = 87Sr/^{86}Sr - {}^{87}Rb/^{86}Sr * (e^{\lambda t} - 1)$, $\lambda_{Rb} = 1.41 * 10^{-11}\ t^{-1}$, $t = 200$ Ma.

again. Then, the F ions were removed from the sample for conversion to chloride. The chloride sample was dissolved with 1 mL of 2 mol/L hydrochloric acid, and Pb was separated by the resin exchange method. After evaporation to dryness, the Pb isotopes were measured by thermal surface ionization mass spectrometry. The laboratory background level of Pb during the whole process was 1×10^{-10} g.

5. Analytical Results

5.1. Microthermometry of Fluid Inclusions. The salinity and homogenisation temperature of primary gas-liquid two-phase fluid inclusions in 13 sphalerite and 51 quartz grains were measured. The results are shown in Table 2. The homogenisation temperature of fluid inclusions in sphalerite ranges from 132.5 to 216.5°C, with an average of 174.4°C; the salinity ranges from 12.39% to 20.67% NaCleqv, with an average of 17.14% NaCleqv. The homogenisation temperature of fluid inclusions in quartz ranges from 130.0 to 275.0°C, with an average of 214.4°C; the salinity ranges from 7.17% to 19.60% NaCleqv, with an average of 13.43% NaCleqv.

5.2. Rb–Sr Isotope Compositions and the Isochron Age. The analysis results are shown in Table 3. All sphalerite samples exhibited Rb and Sr concentrations ranging from 0.01197 to 0.1335 ppm and 0.09629 to 0.2523 ppm, respectively. The $^{87}Rb/^{86}Sr$ ratios varied from 0.3589 to 3.336 (mean = 0.7131 , $n = 5$), and the $^{87}Sr/^{86}Sr$ ratios varied from 0.71950 to 0.72829 (mean = 0.7131, $n = 5$). After excluding the outlier sample LYQ-7, the remaining four sphalerite samples showed a linear correlation on the $^{87}Rb/^{86}Sr$ vs. $^{87}Sr/^{86}Sr$ plots (Figure 5(a)), which corresponded to an isochron age of 209.8 ± 5.2 Ma with an initial $^{87}Sr/^{86}Sr$ ratio of 0.71834 ± 0.00012 and a mean squared weighted deviation (MSWD) of 0.85.

5.3. Sulfur Isotope Compositions. S isotope compositions of sphalerite and pyrite are shown in Table 4. The S isotope compositions of sphalerite were homogeneous, except for an outlier ($\delta^{34}S$ =11.93‰) measured from pyrite (Figure 6). The $\delta^{34}S$ values ranged from -2.62‰ to 1.42‰ with an average of -1.11‰ at the Laoyingqing Pb–Zn deposit, thereby indicating that S may have come from a single source. The $\delta^{34}S$ values of sphalerite in the Laoyingqing Pb–Zn deposit were significantly lower than those of most Pb–Zn deposits in the SYGT (Figure 7).

5.4. Lead Isotope Compositions. The Pb isotopic compositions of the Laoyingqing Pb–Zn deposit are listed in Table 5. The sulfide samples of different ore bodies, ore types, and ore minerals in this deposit have a relatively homogeneous Pb isotopic composition, with $^{206}Pb/^{204}Pb$ ranging from 17.9537 to 18.2907, $^{207}Pb/^{204}Pb$ ranging from 15.6504 to 15.6755, and $^{208}Pb/^{204}Pb$ ranging from 37.9921 to 38.4494; this result indicated that the Pb source was relatively consistent.

The Pb isotopic composition of the Laoyingqing Pb–Zn deposit was different from other major Pb–Zn deposits in the SYGT. The Pb isotopic compositions of the Laoyingqing deposit were comparable to those of the Chipu deposit which extended horizontally as a linear array within the range of the basement rocks. The Pb isotopic compositions of the Huize, Maoping, Maozu, Daliangzi, Tianbaoshan, Tianqiao, Shaojiwan, and Qingshan deposits fell within the Pb isotopic range of Devonian to Permian carbonates and basement rocks and showing the greatest variability in the y-direction on the plot.

6. Discussion

6.1. Timing of the Pb–Zn Mineralisation in the Laoyingqing Deposit. The basic premise of Rb–Sr dating of hydrothermal minerals is to be simultaneous, homologous, closed, with a consistent $^{87}Sr/^{86}Sr$ ratio and a different $^{87}Rb/^{86}Sr$ ratio

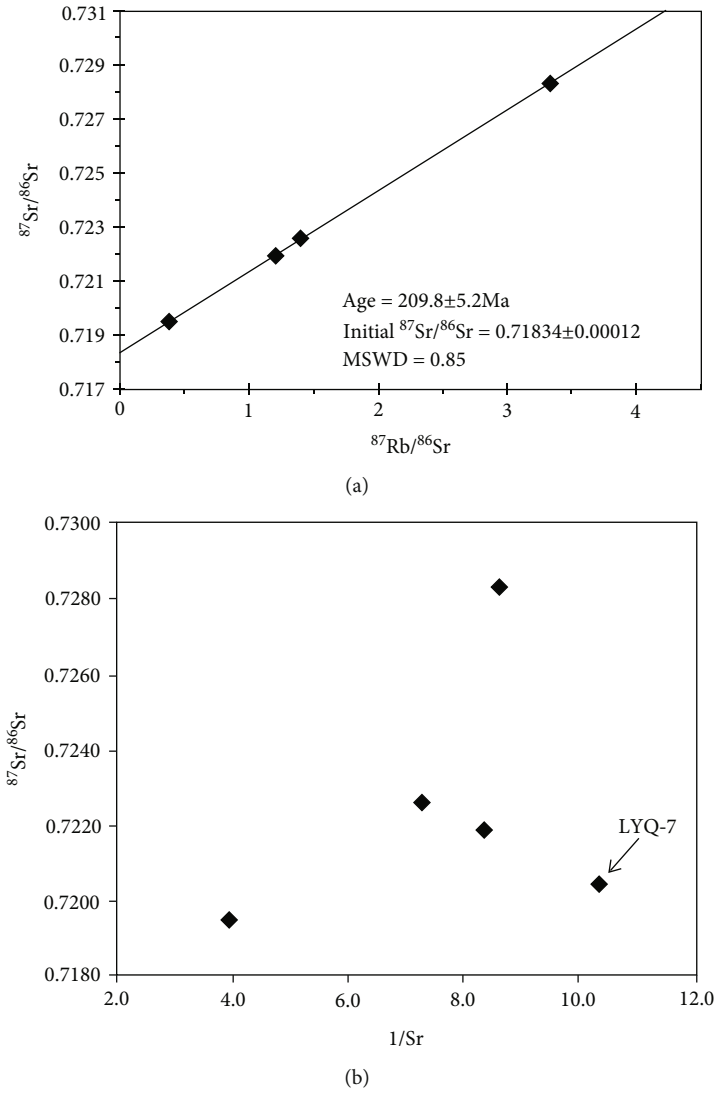

Figure 5: Plot of sulfide Rb–Sr isochron for the Laoyingqing Pb–Zn deposit (a) and plot of sulfide $^{87}Sr/^{86}Sr$ vs. 1/Sr for the Laoyingqing Pb–Zn deposit (b).

Table 4: Sulfur isotopic compositions of sulfides from the Laoyingqing Pb–Zn deposit.

Sample no.	Mineral	$\delta^{34}S_{V\text{-}CDT}$‰	Source
LYQ-1	Sphalerite	0.12	This paper
LYQ-2	Sphalerite	-2.62	
LYQ-3	Sphalerite	-1.87	
LYQ-4-2	Pyrite	11.93	
LYQ-5	Sphalerite	1.42	
LYQ-6	Sphalerite	-1.60	
LYQ-7	Sphalerite	-1.38	
LYQ-8	Sphalerite	-1.86	

[86]. For the medium and low-temperature Pb–Zn deposits, the difference between the homogenisation temperature of the secondary inclusions and the primary inclusions in the minerals was small, complicating the separation of inclusions [15]. During the experiment, both crushing sphalerite to a less than 200 mesh and ultrasonic cleaning greatly diminished the interference of primary and secondary fluid inclusions; thus, the data obtained from the solid residue is more likely to represent the mineralisation age [44, 87]. In this study, dense massive ores from the same ore body and same middle section were selected for analyses. The sphalerite grains had a high purity, with no gangue mineral interpenetration and only a few fractures, which satisfied the precondition of Rb–Sr isotopic dating to the greatest extent. The $^{87}Sr/^{86}Sr$ and 1/Sr ratios of the sphalerite were not linearly correlated (Figure 5(b)), so the isochron (Figure 5(a)) was not a pseudoisochron of two-component mixing. Therefore, the isochron age accurately reflected the timing of the Pb–Zn mineralisation [40, 49, 51, 88]. The Rb–Sr dating of sphalerite in the Laoyingqing Pb–Zn deposit showed that the four samples were all located on the isochron (Figure 5(a)), indicating that the Sr isotopes were homogeneous and the sealing conditions were adequate in the

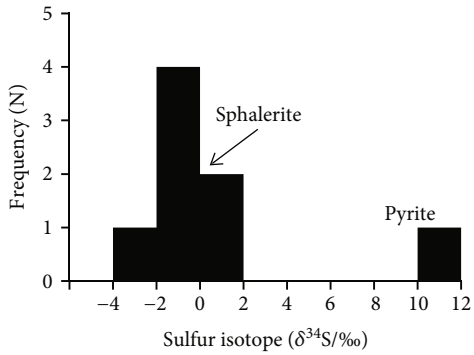

FIGURE 6: Histograms of the sulfur isotopic compositions of sulfides from the Laoyingqing deposit.

process of ore mineral formation; thus, the fitted isochron age had a high accuracy. Nakai et al.[40] interpreted that the previous failure in Rb–Sr dating of sphalerite occurred because either the ore-forming system was not closed or the fluid inclusions in minerals were not cleaned out prior analyses. It is possible that for similar reasons, e.g., interference of fluid inclusions, the sample LYQ-7 in this study did not yield results that fall on the isochron.

Geologically, the Laoyingqing Pb–Zn deposit is located in the secondary fault in the core of the Wuxing anticline and is spatially controlled by the fault-fold structure composed of the Xiaojiang Fault and Wuxing anticline. This implies that the Pb–Zn mineralisation should have occurred earlier than the formation of the Wuxing anticline. However, there is no data to constrain the timing of the formation of the Wuxing anticline. The youngest strata involved in the anticline are the sediments of the Triassic Guanling Formation, which were deposited at 240–230 Ma. Therefore, the formation may provide an upper age limit for the Laoyingqing deposit. Thus, the formation of the Pb–Zn deposits may occur after the deposition of the Guanling Formation. The sphalerite Rb–Sr isochron age (209.8 ± 5.2 Ma) for the Laoyingqing deposit is in accordance with this conclusion. In comparison, geological inferences, structural deformation screening, structural paleo-stress analyses, and isotopic dating[5] infer that the main age of the formation of the thrust-fold structure and ore formation period of the deposits in the SYGT was the late Indosinian (200–230 Ma), and some ore-forming ages of the deposits could be extended to the early Yanshan. The Rb–Sr isochron age of sphalerite in the Laoyingqing Pb–Zn deposit was also consistent with this conclusion.

The Laoyingqing Rb–Sr age is approximately the same as that of most other SYGT Pb–Zn deposits within a reasonable degree of uncertainty (Table 1 and Figure 7; [7, 12, 14, 55, 80, 89]). Although many ages are derived by Rb–Sr isotopic dating, this coincidence not only provides more credibility for the Laoyingqing Rb–Sr date but also indicates that the Rb–Sr geochronology is a suitable dating method for most SYGT Pb–Zn deposits.

The presently available ages of the SYGT Pb–Zn deposits show that most formed between 230 and 190 Ma (Figure 8). The age of the Laoyingqing deposit also falls within in this period, indicating that deposits in the area may have been formed synchronously under the background of a regional hydrothermal event triggered by the orogenic collision event in the late Indosinian ([68, 69, 90]).

6.2. Possible Sources of Sulfur. The composition of S isotopes has always been one of the important methods used to understand the sources of ore-forming materials. An S-source analysis of a deposit must be based on the total S isotope composition in the hydrothermal fluid during sulfide precipitation [92]. Primary ores from the Laoyingqing Pb–Zn deposit were composed primarily of sphalerite, with a small amount of pyrite and galena. The lack of barite and other sulfate minerals in the ores indicated a low oxygen fugacity. Therefore, the δ^{34}S value of sulfide was mostly representative of the total S isotope composition of the hydrothermal fluid, which can be used to directly trace the S source [93].

The Xiaojiang Fault is a regional deep fault, which provides a channel for the flow of fluid in the rocks. The ore mineral assemblage of the Laoyingqing Pb–Zn deposit is simple, and sulfate minerals are not developed in the wall rocks and ore. However, previous studies have shown that sulfate layers developed in the overlying Sinian and Cambrian marine carbonate rocks [6, 52]. The δ^{34}S values of marine sulfate in the Sinian Dengying period of the Yangtze Plate range from 20.2‰ to 38.7‰ [94], and the δ^{34}S values of marine sulfates in phosphorites of the Lower Cambrian Meishucun Formation (Yuhucun Formation) range from 17.4‰ to 33.6‰ [95]. Marine sulfate can form reduced S through bacterial reduction of sulfur (BSR) and TSR [96], providing a sufficient S source for metal deposits.

Generally, BSR mainly occurs at relatively low temperatures (less than 120°C, generally 50–70°C) [97, 98]. The S isotope fractionation caused by BSR is generally 4.0–46.0‰, and the δ^{34}S value of H_2S is generally negative [97]. However, TSR often occurs at relatively high temperatures (above 150°C), and TSR can cause 10–25‰ fractionation between seawater sulfate rock and reduced S at 150°C. With an increase in temperature, $\Delta\delta^{34}$S decreases as follows: at 100°C, $\Delta\delta^{34}S = 20‰$; at 150°C, $\Delta\delta^{34}S = 15‰$; and at 200°C, $\Delta\delta^{34}S = 10‰$ [98–100]. The homogenisation temperature of primary fluid inclusions in sphalerite and quartz grains in the Laoyingqing Pb–Zn deposit ranges from 130 to 275°C, with an average of 206.3°C (Table 2). Therefore, at this temperature, sulfate developed in the overlying marine strata may produce reduced S through TSR, and provide the main S source for the deposit through the fractures.

In the process of mineral precipitation, there is usually no obvious S isotope fractionation between reduced S and metal sulfides. For metal deposits with reduced S provided by TSR, the δ^{34}S value of ore minerals should be approximately 15–20‰ lower than that of seawater sulfate in the formation [13]. The δ^{34}S value of pyrite in the sulfides of the deposit is 11.93‰, approximately 8–26‰ lower than that of marine sulfate in the overlying strata, which is close to the expected S isotope fractionation caused by TSR. However, the δ^{34}S value of sphalerite grains ranges from -2.62‰ to 1.42‰, with an average of -1.11‰, which is 23‰ to 36‰ lower than that of marine sulfate in the overlying strata. The S source may be a contribution of deep mantle-derived S (-3.0‰–+3.0‰) or

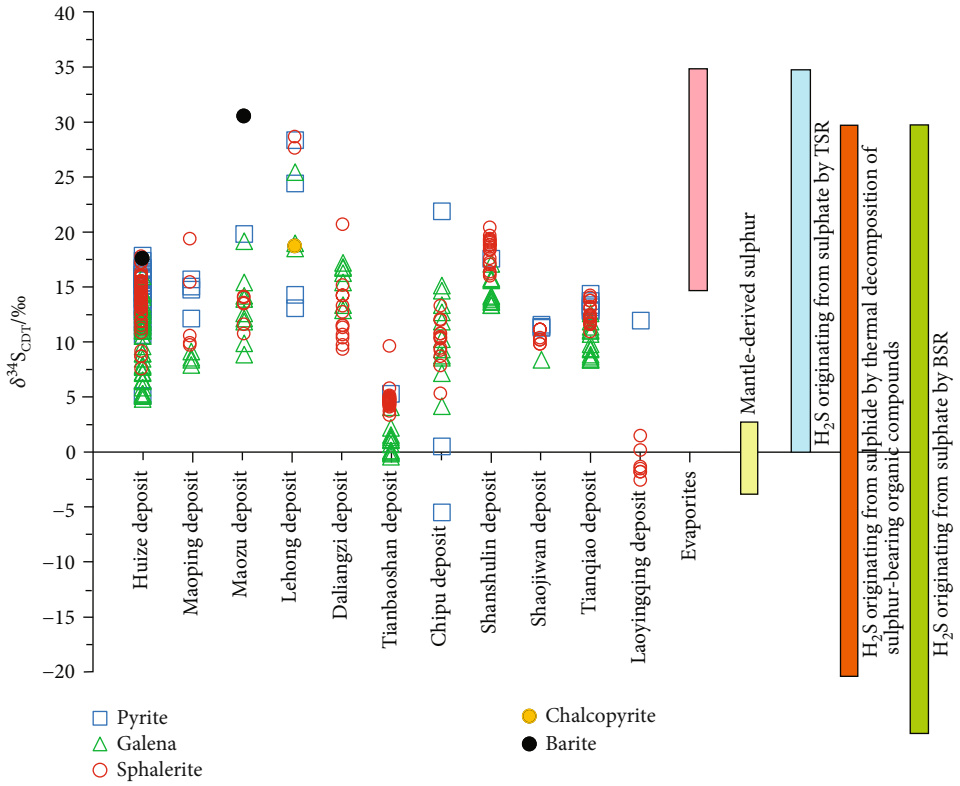

Figure 7: Comparison of sulfur isotopic compositions between the Laoyingqing Pb–Zn deposit and the major deposits in the SYGT (modified from [26]). S isotope compositions of the Huize deposit are taken from Liu and Lin [6], Li et al. [76], Han et al. [52], and Zhang [15]; those of the Maoping deposit are taken from Liu and Lin [6] and Wang et al. [11]; those of the Maozu deposit are taken from Liu and Lin [6], Zhang [15], and Zhou et al. [12]; those of the Lehong deposit are taken from Zhang et al. [14]; those of the Daliangzi deposit are taken from Liu and Lin [6], Zhang [15], Wu [13], and Yuan et al. [77]; those of the Tianbaoshan deposit are taken from Liu and Lin [6], Zhang [15], Zhou et al. [17], Zhu et al. [78], and He et al. [79]; those of the Chipu deposit are taken from Zhang [15] and Wu [13]; those of the Shanshulin deposit are taken from Zhou et al. [54]; those of the Shaojiwan deposit are taken from Zhou et al. [55]; and those of the Tianqiao deposit are taken from Zhou et al. [8].

Table 5: Lead isotopic compositions of sulfides from the Laoyingqing Pb–Zn deposit.

Sample no	Mineral	$^{206}Pb/^{204}Pb$	2σ	$^{207}Pb/^{204}Pb$	2σ	$^{208}Pb/^{204}Pb$	2σ	Source
LYQ-1	Sphalerite	17.9537	0.0004	15.6504	0.0004	37.9921	0.0009	This paper
LYQ-2	Sphalerite	18.2420	0.0003	15.6695	0.0003	38.2857	0.0007	
LYQ-3	Sphalerite	18.2465	0.0004	15.6755	0.0003	38.3679	0.0007	
LYQ-5	Sphalerite	18.0401	0.0003	15.6612	0.0003	38.1092	0.0008	
LYQ-6	Sphalerite	18.2907	0.0004	15.6682	0.0003	38.4494	0.0008	
LYQ-7	Sphalerite	18.1325	0.0004	15.6553	0.0003	38.2107	0.0009	
LYQ-8	Sphalerite	18.1637	0.0003	15.6662	0.0003	38.2751	0.0007	
LYQ-4-2	Pyrite	18.0048	0.0003	15.6562	0.0002	38.0799	0.0006	

organic matter pyrogenic S (Figure 7). However, the main magmatic rocks around the ore district and in the SYGT are the Late Permian Emeishan basalts (256 Ma) [101] and the basic diabase vein (156–166 Ma) [16], with the formation age of the basalt being older than the ore-forming age (209.8 ± 5.2 Ma). The formation age of the diabase vein is younger than the ore-forming age, and no magmatism that coincides with the ore-forming age has been observed. Any other instances of concealed Indosinian magma of unknown depth that can provide mantle-derived S to participate in mineralisation are unknown. However, some studies report that there is a genetic link between the Emeishan basalts and the Pb–Zn deposits, characterised in either providing ore-forming materials or energy transfers [30, 102–104]. Therefore, it cannot be ruled out that the ore-forming fluid activated the Emeishan basalts to provide a small amount of S.

At temperatures higher than 50°C, S-containing organic matter can be thermally decomposed to produce H_2S [59].

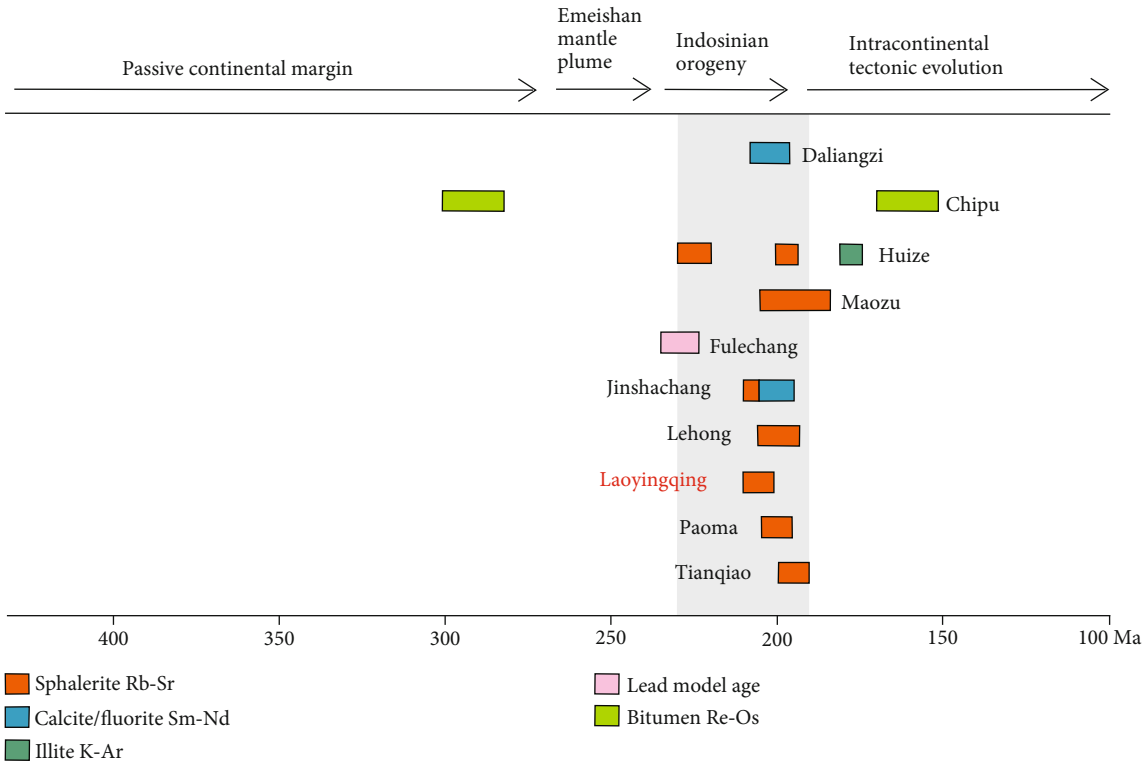

Figure 8: Ages and geological settings of major Pb–Zn deposits in the SYGT (modified from [91]). Sources of the data are taken from Yin et al. [53], Lin et al. [89], Wu [13], Zhou et al. [12], Zhang et al. [14], Zhang et al. [7], Zhou et al. [80], and this study.

The carbonaceous slate of the Kunyang Group contains a large amount of dispersed carbonised S-containing organic matter, and the $\delta^{34}S$ value of organic S is generally negative [18]. The thermal energy provided by the ore-forming hydrothermal fluid causes the pyrolysis of S-containing organic matter in the wall rock to produce reduced S, which is mixed with the reduced S formed by the sulfate in the overlying strata through TSR. This mechanism is different from other Pb–Zn deposits in the SYGT.

Therefore, the reduced S in the sulfide of the Laoyingqing Pb–Zn deposit may have mainly been derived from the mixture of the reduced S produced by the marine sulfate in the overlying strata through TSR and the reduced S produced by the pyrolysis of S-containing organic matter in the carbonaceous slate of the Kunyang group, with a possible addition of a small amount of mantle-derived S at a later stage.

6.3. Possible Sources of Ore-Forming Metals

6.3.1. Pb Isotope Constraints. The Pb isotopic composition of sulfides in the Laoyingqing Pb–Zn deposit is relatively homogeneous which implies that Pb was supplied from either a completely mixed source or a single source. Although the Pb isotope compositions of sulfides vary within a small range, a clear linear trend can be observed on the $^{208}Pb/^{204}Pb$–$^{206}Pb/^{204}Pb$ diagram (Figure 9(b)), which is usually interpreted as a mixed source of Pb [105–107]. The Pb isotopic compositions of all samples plot on the upper crust evolution curve in a nearly EW-trending linear array in the $^{207}Pb/^{204}Pb$ vs. $^{206}Pb/^{204}Pb$ space (Figure 9(a)), thereby indicating that the Pb ore had a predominantly upper crust source, with a possible minor Pb contribution from an orogenic belt.

Most of the Pb–Zn deposits in the SYGT were hosted in carbonate rocks, and large areas of Emeishan basalt distribution and basement rocks (Kunyang and Huili Groups) were exposed in the region. Therefore, most scholars believe that the ore-forming materials were provided by basement rocks, carbonate rocks, and Emeishan basalts; however, their proposed contribution compositions are different as follows: (1) mainly provided by sedimentary rocks, that is carbonate rocks [27]; (2) mainly originating from Precambrian basement rocks [24]; or (3) Emeishan basalt providing the main source of thermal power as well as part of the ore-forming material [102].

The Pb isotopic compositions of sulfides in the Laoyingqing Pb–Zn deposit were different from those of Cambrian sedimentary rocks, basalt, Sinian dolomite, and Devonian to Permian carbonate rocks in this region. However, they were mostly consistent with the basement rock (Kunyang Group) (Table 6). The Pb isotopic compositions of sulfides in the Laoyingqing Pb–Zn deposit showed high consistency with the age-corrected Pb isotopic compositions of the basement rocks, yet minimal consistency with the Devonian to Permian carbonate rocks and the Sinian Dengying Formation of dolomites (Figure 9(a)). This indicated that a mixture of multiple Pb sources may have occurred, that is the Pb ore was largely derived from the basement rocks and the Pb isotopes were homogenised in the ore-forming process. This interpretation supports the argument that the basement rocks provided

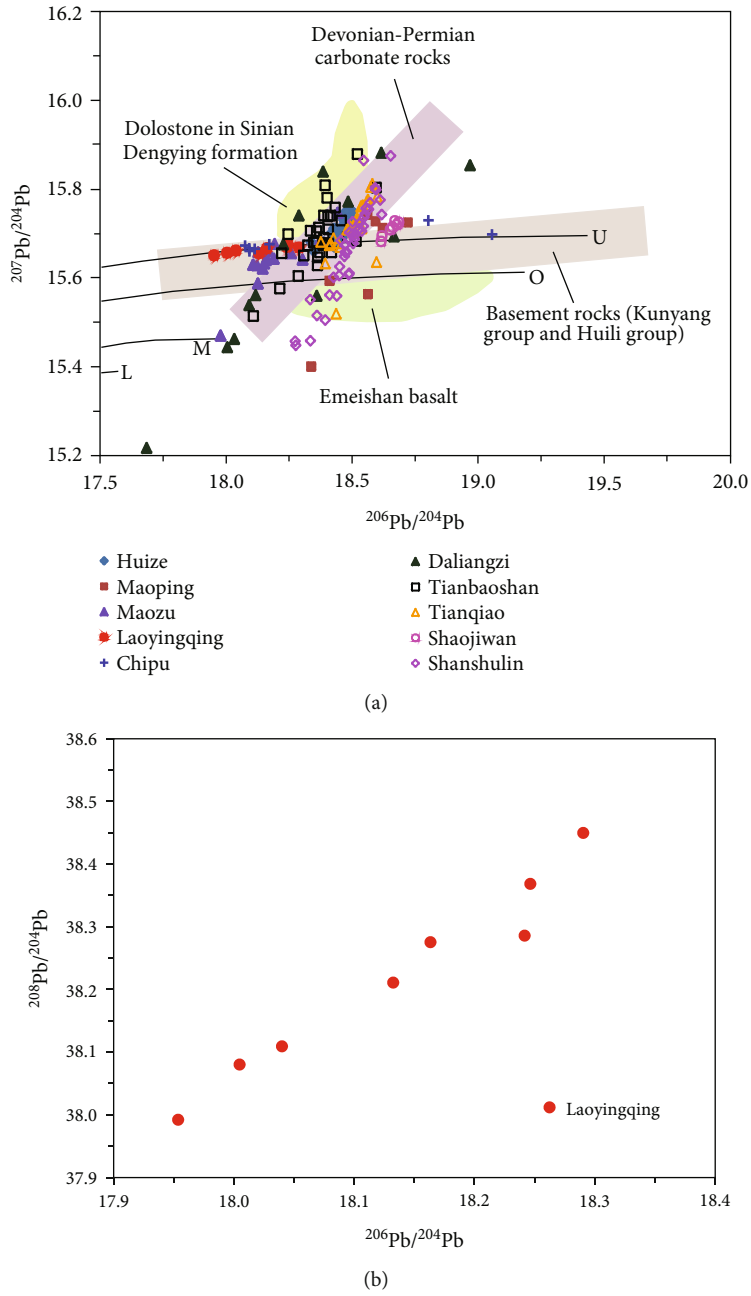

Figure 9: Plots of $^{207}Pb/^{204}Pb$ vs. $^{206}Pb/^{204}Pb$ for the Laoyingqing Pb–Zn deposit (Trends for the upper crust (U), orogen (O), mantle (M), and lower crust (L) are taken from Zartman and Doe [108]) (a) and Plots of $^{208}Pb/^{204}Pb$–$^{206}Pb/^{204}Pb$ for the Laoyingqing Pb–Zn deposit (b). Pb isotope compositions of the Huize deposit are taken from Zhou [109], Han et al. [65], and Li [110]; those of the Maoping deposit are taken from Liu and Lin [6] and Wang et al. [11]; those of the Maozu deposit are taken from Liu and Lin [6] and Zhou et al. [12]; those of the Chipu deposit are taken from Wu [13]; those of the Daliangzi deposit are taken from Zhu et al. [111]; those of the Tianbaoshan deposit are taken from Zhou et al. [17]; those of the Tianqiao deposit are taken from Zhou et al. [8]; those of the Shaojiwan deposit are taken from Zhou et al. [55]; those of the Shanshulin deposit are taken from Zhou et al. [54]. The age-corrected isotopic ranges (200 Ma) for the Sinian (Z) Dengying Formation dolostone, the Devonian to Permian (D–P) carbonates, the Proterozoic basement rocks, and the Emeishan basalts are delineated by the data from Hu [33], Liu and Lin [6], Zhou et al. [24], Han et al. [52], and Yan et al. [84].

ore-forming materials, which is differed from the conclusion that the Pb ore of the majority of other SYGT Pb–Zn deposits was predominantly derived from carbonate rocks.

The age difference between the Emeishan basalt magmatic activity (approximately 260 Ma) and the regional Pb–Zn mineralisation (approximately 200 Ma) may be more than 50 Ma [112, 113], thereby indicating that there is no direct genetic link between the two events. However, the ore-forming fluids likely activated part of the ore-forming metals in Emeishan basalt, especially the ore-forming element Zn, during the processes of atmospheric precipitation or interlayer water infiltration [8].

Table 6: Statistical results of the Pb isotope compositions of the Laoyingqing Pb–Zn deposit, Sinian dolomite, Cambrian sedimentary rocks, Devonian to Permian carbonate rocks, Precambrian basement rocks (Kunyang Group), and Permian Emeishan flood basalts.

Statistical object	Mineral/rock	Number of samples	$(^{206}Pb/^{204}Pb)_{200Ma}$	$(^{207}Pb/^{204}Pb)_{200Ma}$	$(^{208}Pb/^{204}Pb)_{200Ma}$	Source
Laoyingqing Pb–Zn deposit	Sphalerite, pyrite	8	17.9537~18.2907	15.6504~15.6755	37.9921~38.4494	This paper
Cambrian sedimentary rocks		4	20.950~22.354	15.837~15.930	40.878~41.928	Zhou et al. [80]
Sinian Dengying Fm., Dolostone		20	18.198~18.517	15.699~15.987	38.547~39.271	Han et al. [9, 52], Hu [33], Liu and Lin [6], Wang et al. [81–83], Yan et al. [84], Zheng and Wang [85], Zhou et al. [24]
Devonian–Permian carbonate rocks		80	18.120~18.842	15.500~16.522	38.235~39.685	
Precambrian basement rocks (Kunyang Group)		27	17.781–20.993	15.582–15.985	37.178–40.483	
Permian Emeishan flood basalts		56	18.175~19.019	15.528~15.662	38.380~39.928	

Note: $(^{206}Pb/^{204}Pb)_t = (^{206}Pb/^{204}Pb)_p - \mu(e^{\lambda t} - 1)$, $(^{207}Pb/^{204}Pb)_t = (^{207}Pb/^{204}Pb)_p - \mu/137.88(e^{\lambda' t} - 1)$, $(^{208}Pb/^{204}Pb)_t = (^{208}Pb/^{204}Pb)_p - \omega(e^{\lambda'' t} - 1)$, $\lambda = 1.55125 \times 10^{-10}\ t^{-1}$, $\lambda' = 9.8485 \times 10^{-10}\ t^{-1}$, $\lambda'' = 0.49475 \times 10^{-10}\ t^{-1}$, $t = 200$ Ma.

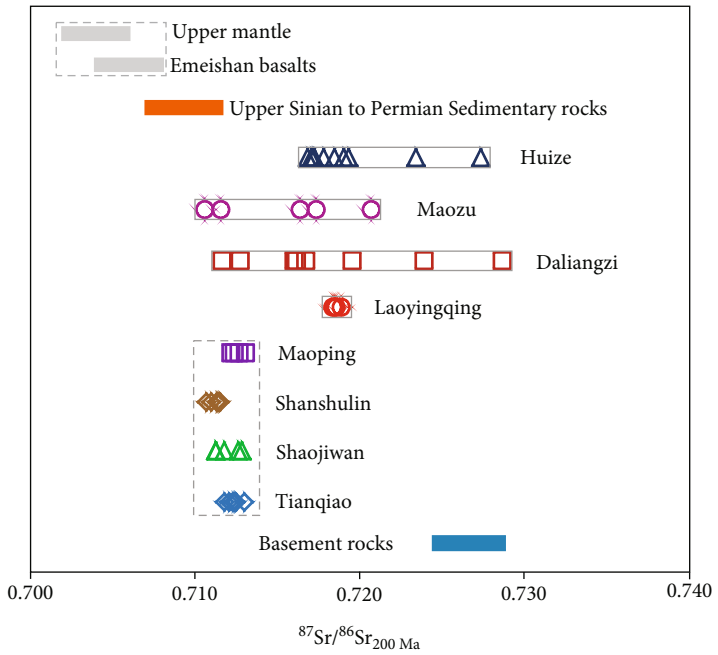

Figure 10: Comparison of $(^{87}Sr/^{86}Sr)_t$ ($t = 200$ Ma) ratios among the major SYGT Pb–Zn deposits, sedimentary rocks, basement rocks, Emeishan basalts, and upper mantle. Sr isotope compositions of the Huize deposit are taken from Yin et al. [53]; those of the Maozu deposit are taken from Zhen et al. (2015); those of the Maoping deposit are taken from Shen et al. [116]; those of the Daliangzi deposit are taken from Zhang et al. [15]; those of the Shanshulin deposit are taken from Zhou et al. [54] and Cheng et al. [115]; those of the Shaojiwan deposit are taken from Zhou et al. [55]; those of the Tianqiao deposit are taken from Zhou et al. [8] and Cheng et al. [115]. The Sr isotopic compositions of the reservoirs are all calculated back to 200 Ma with original data from Faure [117] for the upper mantle; from Huang et al. [102] for the Emeishan basalts; from Deng et al. [32], Hu [33], Zhou et al. [55], and Zhou et al. [54] for the sedimentary rocks; and from Li and Qin [118] and Chen Ran [119] and for the Proterozoic basement rocks.

6.3.2. Constraints from the Sr Isotopes. $^{87}Sr/^{86}Sr$ isotopes are often used to trace the source of ore-forming materials, magmatic fluids, and crust-mantle mixing of deep source fluids [106]. However, when a Sr isotopic composition is used to trace the source of ore-forming fluids/materials, the Sr isotopic composition of potential source areas must be corrected by the ore-forming age. In recent years, considerable progress has been made in the chronology of the Pb–Zn deposits in the SYGT. The results of isotope dating indicate that the deposits in the region were mainly formed in the Late

Triassic–Early Jurassic (approximately 200 Ma). The sphalerite Rb–Sr isochron age of the Laoyingqing Pb–Zn deposit revealed in this study is 209.8 ± 5.2 Ma, which was consistent with this conclusion (Table 1). The age-corrected $^{87}Sr/^{86}Sr$ of four sphalerite samples from the Laoyingqing Pb–Zn deposit range from 0.7184 to 0.7189 (mean = 0.7186), and the initial $^{87}Sr/^{86}Sr$ value is 0.71834. In addition, the age-corrected Sr isotopic compositions of major Pb–Zn deposits such as Huize, Maozu, Maoping, Daliangzi, Shanshulin, Shaojiwan, Tianqiao, Emeishan basalts, hosted sedimentary rocks, and basement rocks in the SYGT are shown in Figure 10.

The initial $^{87}Sr/^{86}Sr$ value of sphalerite in the Laoyingqing Pb–Zn deposit obtained in this study is 0.71834, which is close, albeit slightly lower than the mean continental crust $^{87}Sr/^{86}Sr$ value of 0.719, and higher than the initial mantle Sr value of 0.707 [114]. Therefore, the ore-forming material of this deposit was likely predominantly derived from the continental crust, which is consistent with the Pb isotopic tracer results in this study.

Previous studies have suggested that the source of ore-forming fluids in the SYGT may have flowed through the basement rocks [65, 102], implying they are likely the result of a mixture of basement rocks, sedimentary rocks in different strata, and Emeishan basalt [8, 80, 115]. According to Figure 10, the $(^{87}Sr/^{86}Sr)_{200\ Ma}$ values of the main deposits in the SYGT were significantly higher than the mantle and Emeishan basalt, which seemed to exclude the possibility that the ore-forming materials were completely provided by the mantle and Emeishan basalt. According to several previous geological and geochemical studies on ore deposits, the possibility of the Emeishan mantle plume contributing a large amount of ore-forming materials and fluids has mostly been excluded [8, 36, 120]. The $(^{87}Sr/^{86}Sr)_{200\ Ma}$ value of the main deposits in the SYGT was higher than the Upper Sinian–Permian sedimentary rocks and lower than the basement rocks, thereby suggesting that the ore-forming materials were not entirely derived from the hosted sedimentary rocks or basement rocks. The Laoyingqing, Huize, and Daliangzi deposits all show high $(^{87}Sr/^{86}Sr)_{200Ma}$ values, indicating that Sr was predominantly derived from the basement rocks; in comparison, the $(^{87}Sr/^{86}Sr)_{200Ma}$ values of the Maoping, Shanshulin, Shajiwan, and Tianqiao deposits are more similar to the range (0.7073–0.7111) of the Upper Sinian to Permian carbonate rocks, thereby indicating that Sr was predominantly derived from marine carbonate rocks and less from the basement rocks. At the same time, the initial Sr isotopic values of sphalerite residues in the Laoyingqing, Maoping, Shanshulin, Shaojiwan, and Tianqiao deposits show minimal change, thereby indicating that the Sr isotopes in the ore-forming fluids of each deposit were relatively homogeneous and had the same source. This dynamic may have been detrimental in yielding accurate and reliable Rb–Sr ages of sphalerite.

Therefore, we conclude that the Laoyingqing Pb–Zn deposit has the same characteristics as the major deposits in the SYGT. The main source of metal-rich ore-forming fluids may be predominantly derived from the mixture of the fluid flowing through the basement rock and the fluid flowing through the sedimentary rock of the caprock; however, most of the metal in the ore-forming fluid of the Laoyingqing Pb–Zn deposit is provided by the basement rock, consistent with the Pb isotopic tracer results in this study.

6.4. Possible Ore Genesis and Mineralisation Mechanism

6.4.1. Ore Genesis. The MVT Pb–Zn deposit is a shallow epigenetic deposit that is separated from the dense basin brine at approximately 75–200°C [56]. These deposits occur in the platform carbonate rocks; they are not related to the magmatic activity [56] and are associated with the extensional basin setting [57, 121]. Many previous studies have suggested that the SYGT carbonate-hosted Pb–Zn deposits belong to the MVT considering their similarities in host rocks, tectonic setting, and ore-forming fluids [2, 7, 24, 85, 122]. By comparison (Table 1), the Laoyingqing Pb–Zn deposit may have formed synchronously with most deposits under the background of a regional hydrothermal event triggered by an orogenic collision event in the late Indosinian (~200 Ma) in the SYGT. This deposit demonstrates a series of characteristics that are prevalent in most deposits, such as a clear compressional tectonic setting, ore bodies controlled by a thrust-fold structure, an epigenetic structure, simple ore mineral compositions, vein and lenticular ore bodies, silicification, carbonatisation of wall rocks, and a minimal relationship with magma (Emeishan mantle plume) activity. Moreover, the homogenisation temperature of primary fluid inclusions in sphalerite and quartz grains in the Laoyingqing Pb–Zn deposit ranges from 130 to 275°C, the salinity ranges from 7.17 to 20.67 wt% NaCleqv (Table 2), and the ore-forming fluid is the gas-rich fluid with medium-high temperature and medium-low salinity, which is consistent with most of the SYGT Pb–Zn deposits (fluid inclusion homogenisation temperature ranges from 115 to 280°C, and salinity ranges from 0.9 to 20 wt% NaCleqv; Table 1). Therefore, the origin of the Laoyingqing Pb–Zn deposit is obviously different from the VHMS type and Sedimentary Exhalative type (SEDEX) Pb–Zn deposits, and most likely belongs to the MVT deposits like most deposits in the SYGT.

6.4.2. Ore-Forming Mechanism. The ore-forming mechanism of the deposit should be mainly described in terms of its metal sources, compositional characteristics of fluid components, ability to carry ore-forming metal ions, migration mode, and metal precipitation mechanisms. Therefore, the ore-forming mechanism of the Laoyingqing Pb–Zn deposit can be described as follows. The late Indosinian (~200 Ma) collision orogenic event and the closure of the Tethys Ocean induced a strong oblique strike-slip in the foreland basin on the southwestern margin of the Yangtze Block, forming a large number of thrust nappe fold structures (i.e., Xiaojiang Fault and the Wuxing anticline) [5]. At the same time, large-scale basin brine migrated along regional faults and fissures in the basement and overlying strata, extracted metal elements (such as Pb and Zn), and finally migrated to the basement rocks (Kunyang Group). Simultaneously, extensive hydrothermal flow and circulation reduced S in the sulfate in the overlying strata into thiosulfuric acid and hydrogen sulfuric acid, migrated with the infiltrating fluid, and finally

mixed with the reduced S produced by the pyrolysis of S-containing organic matter in the wall rock (Kunyang group). The thermochemically reduced S of sulfate is the main source of reduced S. When metal-containing fluids and reduced S-containing fluids mixed at favourable fracture sites in the core of the Wuxing anticline, accompanied by changes in ore-forming conditions, metal sulfides precipitated to form ore bodies of industrial value.

Leach et al. [123] calculated the paleomagnetic ages of six major MVT Pb–Zn deposits in North America, and the results showed that the mineralisation process can last for 25 Ma. The S, Pb, and Sr isotope tracing results in this paper cannot entirely exclude the possibility that the Emeishan basalt provided ore-forming metals and reduced sulfur. Therefore, extensive hydrothermal flow may have activated the Emeishan basalt and extracted part of the ore-forming metals or reduced sulfur into the fluid. The ore-forming materials migrated with the infiltration of the fluids and participated in the formation of the ore in the late stage of the ore-forming process.

7. Conclusions

The sphalerite Rb–Sr dating results show that the Laoyingqing Pb–Zn deposit and most of the Pb–Zn deposits in the SYGT were formed at approximately 200 Ma. These deposits are related to the strong regional hydrothermal event triggered by the orogenic collision event in the late Indosinian, and the hydrothermal event had no direct relationship with the Emeishan mantle plume. The low $\delta^{34}S$ value of sphalerites is the result of mixing between reduced S produced by the marine sulfate in the overlying strata through the TSR and reduced S produced by the pyrolysis of S-containing organic matter in the carbonaceous slate of the Kunyang group. Thermochemical reduction of sulfate is the main mechanism for reducing S. However, the addition of a small amount of mantle-derived S in the later period cannot be excluded. The Pb and Sr isotopic compositions indicate that the ore-forming metal was predominantly derived from wall rocks (Kunyang Group) and the contribution of dolomite of the Sinian Dengying Formation and Devonian–Permian carbonate rocks was minimal. It cannot be entirely excluded that the Emeishan basalt provided a small amount of metal elements. This deposit and most of the Pb–Zn deposits in the SYGT belong to the MVT deposits.

Data Availability

The underlying data are already in the manuscript.

Conflicts of Interest

The authors declare that they have no conflicts of interest.

Acknowledgments

This work was financially supported by the National Science Foundation of China (41572060, U1133602), Yunling scholars (2015), Projects of YMLab (2010), and Innovation Team of Yunnan province (2012). We thank Wang Shengkai and Guo Zhonglin of Yunnan Chihong Zn and Ge Co. Ltd. for their strong support and help in fieldwork.

References

[1] R. Z. Hu, T. W. Chen, D. R. Xu, and M. F. Zhou, "Reviews and new metallogenic models of mineral deposits in South China: an introduction," *Journal of Asian Earth Sciences*, vol. 137, pp. 1–8, 2017.

[2] R. Z. Hu, S. Fu, Y. Huang et al., "The giant South China Mesozoic low-temperature metallogenic domain: reviews and a new geodynamic model," *Journal of Asian Earth Sciences*, vol. 137, pp. 9–34, 2017.

[3] C. Y. Li, "Some geological characteristics of concentrated distribution area of epithermal deposits in China," *Earth Science Frontiers*, vol. 6, pp. 163–170, 1999.

[4] G. C. Tu, *The Low Temperature Geochemistry*, Science Press, Beijing, 1998.

[5] R. S. Han, F. Wang, Y. Z. Hu et al., "Metallogenic tectonic dynamics and chronology constrains on the Huize-type (HZT) germanium-rich silver–zinc–lead deposits," *Geotectonica et Metallogenia*, vol. 38, no. 4, pp. 758–771, 2014.

[6] H. C. Liu and W. D. Lin, *Study on the Law of Pb–Zn–Ag Ore Deposit in Northeast Yunnan, China*, Yunnan University Press, Kunming, 1999.

[7] C. Q. Zhang, Y. Wu, L. Hou, and J. W. Mao, "Geodynamic setting of mineralization of Mississippi Valley-type deposits in world-class Sichuan-Yunnan-Guizhou Zn-Pb triangle, southwest China: Implications from age-dating studies in the past decade and the Sm-Nd age of Jinshachang deposit," *Journal of Asian Earth Sciences*, vol. 103, pp. 103–114, 2015.

[8] J. X. Zhou, Z. L. Huang, M. F. Zhou, X. B. Li, and Z. G. Jin, "Constraints of C-O-S-Pb isotope compositions and Rb-Sr isotopic age on the origin of the Tianqiao carbonate-hosted Pb-Zn deposit, SW China," *Ore Geology Reviews*, vol. 53, no. 8, pp. 77–92, 2013.

[9] R. S. Han, Y. Z. Hu, X. K. Wang et al., "Mineralisation model of rich Ge–Ag bearing Zn–Pb polymetallic deposit concentrated district in northeastern Yunnan, China," *Acta Geologica Sinica*, vol. 86, pp. 280–294, 2012.

[10] R. S. Han, H. J. Zou, B. Hu, Y. Z. Hu, and C. D. Xue, "Features of fluid inclusions and sources of ore-forming fluid in the Maoping carbonate-hosted Zn–Pb–(Ag–Ge) deposit, Yunnan, China," *Acta Petrologica Sinica*, vol. 23, no. 9, pp. 2109–2118, 2007.

[11] C. W. Wang, Y. Li, H. Y. Luo, and X. L. Liu, "Genesis of Maoping Pb-Zn deposit in Yunnan Province," *Journal of Kunming University of Science and Technology (Science and Technology)*, vol. 34, no. 1, pp. 7–11, 2009.

[12] J. X. Zhou, Z. L. Huang, and Z. F. Yan, "The origin of the Maozu carbonate-hosted Pb-Zn deposit, southwest China: Constrained by C-O-S-Pb isotopic compositions and Sm-Nd isotopic age," *Journal of Asian Earth Sciences*, vol. 73, pp. 39–47, 2013.

[13] Y. Wu, *The Age and Ore-Forming Process of MVT Deposits in the Boundary Area of Sichuan–Yunnan–Guizhou Provinces, Southwest China*, China University of Geosciences, Beijing, 2013.

[14] Y. X. Zhang, Y. Wu, G. Tian et al., "Mineralisation age and the source of ore-forming material at Lehong Pb–Zn deposit,

Yunnan Province: constraints from Rb–Sb and S isotopes system," *Acta Mineralogica Sinica*, vol. 34, no. 3, pp. 305–311, 2014.

[15] C. Q. Zhang, X. H. Li, J. J. Yu, J. W. Mao, F. K. Chen, and H. M. Li, "Rb–Sr dating of single sphalerites from the Daliangzi Pb–Zn deposit, Sichuan, and its geological significances," *Geological Review*, vol. 54, pp. 532–538, 2008.

[16] R. Wang, C. Q. Zhang, Y. Wu, and C. Wei, "Formation age of the diabase dike in the Tianbaoshan Pb–Zn deposit, Sichuan and its relationships with the Pb–Zn mineralisation," *Mineral Deposits*, vol. 31, pp. 449-450, 2012.

[17] J. X. Zhou, J. G. Gao, D. Chen, and X. K. Liu, "Ore genesis of the Tianbaoshan carbonate-hosted Pb–Zn deposit, Southwest China: geologic and isotopic (C–H–O–S–Pb) evidence," *International Geology Review*, vol. 55, no. 10, pp. 1300–1310, 2013.

[18] Y. Wu, C. Q. Zhang, J. W. Mao, H. G. Ouyang, and J. Sun, "The genetic relationship between hydrocarbon systems and Mississippi Valley-type Zn–Pb deposits along the SW margin of Sichuan Basin, China," *International Geology Review*, vol. 55, no. 8, pp. 941–957, 2012.

[19] S. J. Chen, "A discussion on the sedimentary origin of Pb–Zn deposits in western Guizhou and northeastern Yunnan," *Journal of Guizhou Geology*, vol. 8, no. 3, pp. 35–39, 1984.

[20] W. Liao, "A discussion on the S and Pb isotopic composition characteristics and metallogenic model of the Pb–Zn ore zones in eastern Yunnan and western Guizhou," *Journal of Geology and Exploration*, vol. 1, pp. 1–6, 1984.

[21] J. Z. Wang, C. Y. Li, Z. Q. Li, and J. J. Liu, "The comparison of mississippi valley-type lead-zinc deposits in Southwest of China and in mid-continent of United States," *Bulletin of Mineralogy, Petrology and Geochemistry*, vol. 21, pp. 127–132, 2002.

[22] C. Q. Zhang, J. W. Mao, S. P. Wu et al., "Distribution, characteristics and genesis of MVT lead–zinc deposit in Sichuan–Yunnan–Guizhou provinces," *Mineral Deposits*, vol. 24, no. 3, pp. 336–348, 2005.

[23] W. J. Zhang, "A preliminary discussion on the sedimentary origin and metallogenic rule of Pb–Zn deposits in northeastern Yunnan," *Journal of Geology and Exploration*, vol. 7, pp. 11–16, 1984.

[24] C. X. Zhou, S. S. Wei, J. Y. Guo, and C. Y. Li, "The source of metals in the Qilinchang Zn-Pb deposit, northeastern Yunnan, China: Pb-Sr isotope constraints," *Economic Geology*, vol. 96, no. 3, pp. 583–598, 2001.

[25] C. Q. Zhang, *The Genetic Model of Mississippi Valley–Type Deposits in the Boundary Area of Sichuan, Yunnan and Guizhou Provinces, China, [PhD thesis]*, Chinese Academy of Geological Sciences, 2008.

[26] Z. G. Kong, Y. Wu, F. Zhang, C. Q. Zhang, and X. Y. Meng, "Sources of ore-forming material of typical Pb–Zn deposits in the Sichuan–Yunnan–Guizhou metallogenic province: constraints from the S–Pb isotopic compositions," *Earth Science Frontiers*, vol. 25, pp. 125–137, 2018.

[27] X. B. Li, Z. L. Huang, W. B. Li, Z. L. Zhang, and Z. F. Yan, "Sulfur isotopic compositions of the Huize super-large Pb-Zn deposit, Yunnan Province, China: implications for the source of sulfur in the ore-forming fluids," *Journal of Geochemical Exploration*, vol. 89, no. 1-3, pp. 227–230, 2006.

[28] W. H. Liu, J. Zhang, and J. Wang, "Sulfur isotope analysis of carbonate-hosted Zn-Pb deposits in northwestern Guizhou Province, Southwest China: implications for the source of reduced sulfur," *Journal of Geochemical Exploration*, vol. 181, pp. 31–44, 2017.

[29] J. X. Zhou, K. Luo, X. C. Wang et al., "Ore genesis of the Fule Pb Zn deposit and its relationship with the Emeishan Large Igneous Province: evidence from mineralogy, bulk C O S and in situ S Pb isotopes," *Gondwana Research*, vol. 54, pp. 161–179, 2018.

[30] J. X. Zhou, Z. Z. Xiang, M. F. Zhou et al., "The giant Upper Yangtze Pb-Zn province in SW China: reviews, new advances and a new genetic model," *Journal of Asian Earth Sciences*, vol. 154, pp. 280–315, 2018.

[31] R. H. Zheng, J. G. Gao, H. L. Nian, and F. J. Jia, "Rb–Sr isotopic compositions of sphalerite and its geological implications for Maozu Pb–Zn deposit, Northeast Yunnan Province, China," *Acta Mineralogica Sinica*, vol. 35, no. 4, pp. 435–438, 2015.

[32] H. L. Deng, C. Y. Li, G. Z. Tu, Y. M. Zhou, and C. W. Wang, "Strontium isotope geochemistry of the Lemachang independent silver ore deposit, northeastern Yunnan, China," *Science in China Series D: Earth Sciences*, vol. 29, no. 6, pp. 496–503, 2000.

[33] Y. G. Hu, *Ag Occurrence, Source of Ore-Forming Metals and Mechanism of Yinchangpo Ag–Pb–Zn Deposit, Guizhou*, Institute of Geochemistry, CAS, 1999.

[34] F. C. Lin, "Geological and geochemical characteristics and genesis of supper-large-scale sedex-type stratiform lead–zinc deposits in the Dadu River valley on the western margin of the Yangtze craton," *Acta Geologica Sinica*, vol. 79, no. 4, pp. 540–558, 2005.

[35] S. G. Liu, W. M. Huang, C. H. Chen et al., "Primary study on hydrothermal fluids activities and their effectiveness on petroleum and mineral accumulation of Simian system-Palaeozoic in Sichuan basin," *Journal of Mineralogy and Petrology*, vol. 28, no. 3, pp. 41–50, 2008.

[36] W. B. Li, Z. L. Huang, and M. Yin, "Dating of the giant Huize Zn–Pb ore field of Yunnan Province, Southwest China: constraints from the Sm–Nd system in hydrothermal calcite," *Resource Geology*, vol. 57, no. 1, pp. 90–97, 2007.

[37] S. Nakai, A. N. Halliday, S. E. Kesler, and H. D. Jones, "Rb-Sr dating of sphalerites from Tennessee and the genesis of Mississippi Valley type ore deposits," *Nature*, vol. 346, no. 6282, pp. 354–357, 1990.

[38] D. F. Sangster, *Mississippi Valley-Type Lead–Zinc*, 1996, Geological Survey of Canada.

[39] J. N. Christensen, A. N. Halliday, J. R. Vearncombe, and S. E. Kesler, "Testing models of large-scale crustal fluid flow using direct dating of sulfides; Rb-Sr evidence for early dewatering and formation of mississippi valley-type deposits, Canning Basin, Australia," *Economic Geology*, vol. 90, no. 4, pp. 877–884, 1995.

[40] S. I. Nakai, A. N. Halliday, S. E. Kesler, H. D. Jones, J. R. Kyle, and T. E. Lane, "Rb-Sr dating of sphalerites from Mississippi Valley-type (MVT) ore deposits," *Geochimica et Cosmochimica Acta*, vol. 57, no. 2, pp. 417–427, 1993.

[41] J. Nelson, S. Paradis, J. Christensen, and J. Gabites, "Canadian cordilleran Mississippi Valley-type deposits: a case for Devonian–Mississippian back-arc hydrothermal origin," *Economic Geology and the Bulletin of the Society of Economic Geologists*, vol. 97, no. 5, pp. 1013–1036, 2002.

[42] J. Ostendorf, F. Henjes-Kunst, J. Schneider, F. Melcher, and J. Gutzmer, "Genesis of the carbonate-hosted tres marias

Zn–Pb–(Ge) deposit, Mexico: constraints from Rb–Sr sphalerite geochronology and Pb isotopes," *Economic Geology*, vol. 112, no. 5, pp. 1075–1088, 2017.

[43] J. Schneider, F. Melcher, and M. Brauns, "Concordant ages for the giant Kipushi base metal deposit (DR Congo) from direct Rb–Sr and Re–Os dating of sulfides," *Mineralium Deposita*, vol. 42, no. 7, pp. 791–797, 2007.

[44] T. Pettke and L. W. Diamond, "RbSr isotopic analysis of fluid inclusions in quartz: evaluation of bulk extraction procedures and geochronometer systematics using synthetic fluid inclusions," *Geochimica et Cosmochimica Acta*, vol. 59, no. 19, pp. 4009–4027, 1995.

[45] J. C. Brannon, F. A. Podosek, and S. C. Cole, "*Radiometric dating of Mississippi Valley-type ore deposits*," in *Carbonate-Hosted Lead-Zinc Deposits: 75th Anniversary Volume*, Special Publications of the Society of Economic Geologists, 1996.

[46] D. C. Bradley, D. L. Leach, D. Symons et al., "Reply to discussion on "tectonic controls of Mississippi valley-type lead-zinc mineralisation in orogenic forelands" by S.E. Kesler, J.T. Christensen, R.D. Hagni, W. Heijlen, J.R. Kyle, K.C. Misra, P. Muchez, and R. van der Voo Mineralium Deposita," *Mineralium Deposita*, vol. 39, pp. 515–519, 2004.

[47] L. Cao, Q. F. Duan, and Y. Zhou, "Rb–Sr dating of sphalerites from the Aozigang zinc deposit in Hubei Province and its geological significance," *Geology in China*, vol. 42, pp. 235–247, 2015.

[48] C. X. Feng, S. Liu, X. W. Bi et al., "An investigation of metallogenic chronology of eastern ore block in Baiyangping Pb–Zn–Cu–Ag polylmetallic ore deposit, Lanping Basin, western Yunnan Province," *Mineral Deposits*, vol. 36, pp. 691–704, 2017.

[49] D. Rosa, J. Schneider, and M. Chiaradia, "Timing and metal sources for carbonate-hosted Zn-Pb mineralization in the Franklinian Basin (North Greenland): Constraints from Rb-Sr and Pb isotopes," *Ore Geology Reviews*, vol. 79, pp. 392–407, 2016.

[50] S. H. Tian, Y. Gong, Z. Yang et al., "Rb–Sr and Sm–Nd isochron ages of the dongmozhazhua and mohailaheng Pb–Zn ore deposits in the Yushu area, southern Qinghai and their geological implications," *Acta Geologica Sinica*, vol. 88, no. 2, pp. 558–569, 2014.

[51] S. F. Xiong, Y. J. Gong, S. Y. Jiang, X. J. Zhang, Q. Li, and G. P. Zeng, "Ore genesis of the Wusihe carbonate-hosted Zn-Pb deposit in the Dadu River Valley district, Yangtze Block, SW China: evidence from ore geology, S-Pb isotopes, and sphalerite Rb-Sr dating," *Mineralium Deposita*, vol. 53, pp. 967–979, 2018.

[52] R. S. Han, C. Q. Liu, Z. L. Huang et al., "Geological features and origin of the Huize carbonate-hosted Zn-Pb-(Ag) District, Yunnan, South China," *Ore Geology Reviews*, vol. 31, no. 1-4, pp. 360–383, 2007.

[53] M. D. Yin, W. B. Li, and X. W. Sun, "Rb–Sr isotopic dating of sphalerite from the giant Huize Zn–Pb ore field, Yunnan Province, Southwestern China," *Chinese Journal of Geochemistry*, vol. 28, no. 1, pp. 70–75, 2009.

[54] J. X. Zhou, Z. L. Huang, Z. C. Lv, X. K. Zhu, J. G. Gao, and H. Mirnejad, "Geology, isotope geochemistry and ore genesis of the Shanshulin carbonate- hosted Pb-Zn deposit, southwest China," *Ore Geology Reviews*, vol. 63, pp. 209–225, 2014.

[55] J. X. Zhou, Z. L. Huang, and G. P. Bao, "Geological and sulfur-lead-strontium isotopic studies of the Shaojiwan Pb-Zn deposit, southwest China: Implications for the origin of hydrothermal fluids," *Journal of Geochemical Exploration*, vol. 128, pp. 51–61, 2013.

[56] D. L. Leach and D. F. Sangster, "Mississippi Valley-type lead–zinc deposits," in *Mineral Deposit Models*, R. V. Kirkham, Ed., pp. 289–314, Geological Association of Canada Special Paper, 1993.

[57] D. L. Leach, D. F. Sangster, K. D. Kelley et al., "Sediment-hosted zinc–lead deposits: a global perspective," *Economic Geology*, vol. 100, pp. 561–607, 2005.

[58] M. Tillberg, H. Drake, T. Zack, E. Kooijman, M. J. Whitehouse, and M. E. Åström, "*In situ* Rb-Sr dating of slickenfibres in deep crystalline basement faults," *Scientific Reports*, vol. 10, no. 1, p. 562, 2020.

[59] N. I. Basuki, B. E. Taylor, and E. T. C. Spooner, "Sulfur isotope evidence for thermochemical reduction of dissolved sulfate in Mississippi Valley-type zinc-lead mineralization, Bongara area, northern Peru," *Economic Geology*, vol. 103, no. 4, pp. 783–799, 2008.

[60] H. Mirnejad, A. Simonetti, and F. Molasalehi, "Pb isotopic compositions of some Zn-Pb deposits and occurrences from Urumieh- Dokhtar and Sanandaj-Sirjan zones in Iran," *Ore Geology Reviews*, vol. 39, no. 4, pp. 181–187, 2011.

[61] S. G. Sebastian Staude, K. Pfaff, F. Ströbele, W. R. Premo, and G. Markl, "Deciphering fluid sources of hydrothermal systems: a combined Sr- and S-isotope study on barite (Schwarzwald, SW Germany)," *Chemical Geology*, vol. 286, no. 1-2, pp. 1–20, 2011.

[62] Y. Tang, X. Bi, M. Fayek et al., "Genesis of the Jinding Zn-Pb deposit, northwest Yunnan Province, China: Constraints from rare earth elements and noble gas isotopes," *Ore Geology Reviews*, vol. 90, pp. 970–986, 2017.

[63] Z. B. Zhang, C. Y. Li, G. C. Tu, B. Xia, and Z. Q. Wei, "Geotectonic evolution background and ore-forming process of Pb–Zn deposits in Chuan–Dian–Qian area of Southwest China," *Geotectonica an Metallogenia*, vol. 30, no. 3, pp. 343–354, 2006.

[64] R. S. Han, C. Q. Liu, Z. L. Huang, J. Chen, D. Y. Ma, and Y. Li, "Study on the metallogenic model of the Huize Pb–Zn deposit in Yunnan Province," *Acta Mineralogica Sinica*, vol. 21, pp. 674–680, 2001.

[65] R. S. Han, J. Chen, Z. L. Huang, D. Y. Ma, C. D. Xue, and Y. Li, *Dynamics of Tectonic Ore-Forming Processes and Localization-Prognosis of Concealed Orebodies-as Exemplified by the Huize Super-Large Zn–Pb–(Ag–Ge) District, Yunnan*, Science Press, Beijing, 2006.

[66] W. H. Sun, M. F. Zhou, J. F. Gao, Y. H. Yang, X. F. Zhao, and J. H. Zhao, "Detrital zircon U-Pb geochronological and Lu-Hf isotopic constraints on the Precambrian magmatic and crustal evolution of the western Yangtze Block, SW China," *Precambrian Research*, vol. 172, no. 1-2, pp. 99–126, 2009.

[67] X. F. Zhao, M. F. Zhou, J. F. Li et al., "Late Paleoproterozoic to early Mesoproterozoic Dongchuan Group in Yunnan, SW China: implications for tectonic evolution of the Yangtze block," *Precambrian Research*, vol. 182, no. 1-2, pp. 57–69, 2010.

[68] M. Faure, C. Lepvrier, N. Vuong Van, V. Tich Van, W. Lin, and Z. Chen, "The South China block-Indochina collision: where, when, and how?," *Journal of Asian Earth Sciences*, vol. 79, pp. 260–274, 2014.

[69] L. Qiu, D. P. Yan, W. X. Yang, J. Wang, X. Tang, and S. Ariser, "Early to middle Triassic sedimentary records in

the Youjiang Basin, South China: implications for Indosinian orogenesis," *Journal of Asian Earth Sciences*, vol. 141, pp. 125–139, 2017.

[70] H. Maluski, C. Lepvrier, L. Jolivet et al., "Ar-Ar and fission-track ages in the Song Chay Massif: early Triassic and Cenozoic tectonics in northern Vietnam," *Journal of Asian Earth Sciences*, vol. 19, no. 1-2, pp. 233–248, 2001.

[71] B. Xia, H. Y. Liu, and Y. Q. Zhang, "SHRIMP dating of agpaitic alkalic rocks in Panxi rift zone and its geological implications—examples for Hongge, Baima and Jijie rock bodies," *Geotectonica et Metallogenia*, vol. 28, pp. 149–154, 2004.

[72] D. P. Yan, M. Zhou, C. Y. Wang, and B. Xia, "Structural and geochronological constraints on the tectonic evolution of the Dulong-Song Chay tectonic dome in Yunnan province, SW China," *Journal of Asian Earth Sciences*, vol. 28, no. 4-6, pp. 332–353, 2006.

[73] Y. X. Wang, J. D. Yang, X. C. Tao, and H. M. Li, "The study of the Sm–Nd method for fossil mineral rock and its application," *Journal of Nanjing University*, vol. 24, pp. 297–308, 1988.

[74] Y. X. Wang, J. D. Yang, J. Chen, K. J. Zhang, and W. B. Rao, "The Sr and Nd isotopic variations of the Chinese Loess Plateau during the past 7 Ma: implications for the East Asian winter monsoon and source areas of loess," *Palaeogeography Palaeoclimatology Palaeoecology*, vol. 249, no. 3-4, pp. 351–361, 2007.

[75] R. K. Ludwig, *Isoplot/EX rev. 3.32: a geochronological toolkit for microsoft excel*, Berkeley Geochronology Center, Special Publication 4, Berkeley, 2005.

[76] W. B. Li, Z. L. Huang, and G. Zhang, "Sources of the ore metals of the Huize ore field in Yunnan Province: constrains from Pb, S, C, O and Sr isotope geochemistry," *Acta Petologica Sinica*, vol. 22, no. 10, pp. 2567–2580, 2006.

[77] B. Yuan, J. W. Mao, X. H. Yan, Y. Wu, F. Zhang, and L. L. Zhao, "Sources of metallogenic materials and metallogenic mechanism of Daliangzi ore field in Sichuan Province: constraints from geochemistry of S, C, H, O, Sr isotope and trace element in sphalerite," *Acta Petrologica Sinica*, vol. 30, no. 1, pp. 209–220, 2014.

[78] C. W. Zhu, H. J. Wen, Y. X. Zhang, and H. F. Fan, "Cadmium and sulfur isotopic compositions of the Tianbaoshan Zn-Pb-Cd deposit, Sichuan Province, China," *Ore Geology Reviews*, vol. 76, pp. 152–162, 2016.

[79] C. Z. He, C. Y. Xiao, H. J. Wen, T. Zhou, and C. W. Zhu, "Zn–S isotopic compositions of the Tianbaoshan carbonate-hosted Pb–Zn deposit in Sichuan, China: implications for the source of ore components," *Acta Petrologica Sinica*, vol. 32, no. 11, pp. 3394–3406, 2016.

[80] J. X. Zhou, J. H. Bai, Z. L. Huang, D. Zhu, Z. F. Yan, and Z. C. Lv, "Geology, isotope geochemistry and geochronology of the Jinshachang carbonate- hosted Pb-Zn deposit, southwest China," *Journal of Asian Earth Sciences*, vol. 98, pp. 272–284, 2015.

[81] X. C. Wang, Z. R. Zheng, M. H. Zheng, and X. H. Xu, "Metallogenic mechanism of the Tianbaoshan Pb-Zn deposit, Sichuan," *Chinese Journal of Geochemistry*, vol. 19, no. 2, pp. 121–133, 2000.

[82] J. Z. Wang, Z. Q. Li, and S. J. Ni, "Origin of ore-forming fluids of Mississippi Valley type (MVT) Pb–Zn deposits in Kangdian area, China," *Chinese Journal of Geochemistry*, vol. 22, pp. 369–376, 2003.

[83] C. M. Wang, J. Deng, S. T. Zhang et al., "Sediment-hosted Pb–Zn deposits in southwest Sanjiang Tethys and Kangdian area on the western margin of Yangtze Craton," *Acta Geologica Sinica-English Edition*, vol. 84, pp. 1428–1438, 2010.

[84] Z. F. Yan, Z. L. Huang, C. Xu, M. Chen, and Z. L. Zhang, "Signatures of the source for the Emeishan flood basalts in the Ertan area: Pb isotope evidence," *Chinese Journal of Geochemistry*, vol. 26, no. 2, pp. 207–213, 2007.

[85] M. H. Zheng and X. C. Wang, "Ore genesis of the Daliangzi Pb-Zn deposit in Sichuan, China," *Economic Geology*, vol. 86, no. 4, pp. 831–846, 1991.

[86] W. B. Li, Z. L. Huang, D. R. Xu, J. Cheng, C. Xu, and T. Guan, "Rb–Sr isotopic method on zinc–lead ore deposits: a review," *Geotectonica et Metallogenic*, vol. 26, no. 4, pp. 436–441, 2002.

[87] J. M. Liu, S. R. Zhao, J. Shen, N. Jiang, and W. G. Huo, "Review on direct isotopic dating of hydrothermal ore-forming processes," *Progress in Geophysics*, vol. 13, pp. 46–55, 1998.

[88] J. Schneider, U. Haack, and K. Stedingk, "Rb-sr dating of epithermal vein mineralization stages in the eastern Harz Mountains (Germany) by paleomixing lines," *Geochimica et Cosmochimica Acta*, vol. 67, no. 10, pp. 1803–1819, 2003.

[89] Z. Y. Lin, D. H. Wang, and C. Q. Zhang, "Rb–Sr isotopic age of sphalerite from the Paoma lead–zinc deposit in Sichuan Province and its implications," *Geology in China*, vol. 37, pp. 488–1196, 2010.

[90] Y. Wang, A. Zhang, W. Fan et al., "Petrogenesis of late Triassic post-collisional basaltic rocks of the Lancangjiang tectonic zone, Southwest China, and tectonic implications for the evolution of the eastern Paleotethys: geochronological and geochemical constraints," *Lithos*, vol. 120, no. 3-4, pp. 529–546, 2010.

[91] Y. Y. Tang, X. W. Bi, J. X. Zhou et al., "Rb-Sr isotopic age, S-Pb-Sr isotopic compositions and genesis of the ca. 200 Ma Yunluheba Pb-Zn deposit in NW Guizhou Province, SW China," *Journal of Asian Earth Sciences*, vol. 185, p. 104054, 2019.

[92] H. Ohmoto and R. O. Rye, "Isotopes of sulfur and carbon," in *Geochemistry of Hydrothermal Ore Deposits*, H. L. Barnes, Ed., p. 798, Wiley and Sons, Inc., New York, 2nd edition, 1979.

[93] H. Ohmoto, "Systematics of sulfur and carbon isotopes in hydrothermal ore deposits," *Economic Geology*, vol. 67, no. 5, pp. 551–578, 1972.

[94] T. G. Zhang, X. L. Chu, Q. R. Zhang, L. J. Feng, and W. G. Huo, "The sulfur and carbon isotopic records in carbonates of the Dengying Formation in the Yangtze platform, China," *Acta Petrologica Sinica*, vol. 20, no. 3, pp. 717–724, 2004.

[95] G. A. Shields, H. Strauss, and S. S. Howe, "Sulphur isotope compositions of sedimentary phosphorites from the basal Cambrian of China: implications for Neoproterozoic-Cambrian biogeochemical cycling," *Journal of the Geological Society*, vol. 156, no. 5, pp. 943–955, 1999.

[96] H. Ohmoto, "Stable isotope geochemistry of ore deposits," *Reviews in Mineralogy*, vol. 16, no. 1, pp. 491–560, 1986.

[97] X. Chen and C. J. Xue, "Origin of H_2S in Uragen large-scale Zn–Pb mineralisation, western Tien Shan: bacteriogenic structure and S-isotopic constraints," *Acta Petrologica Sinica*, vol. 32, no. 5, pp. 1301–1314, 2016.

[98] H. G. Machel, H. R. Krouse, and R. Sassen, "Products and distinguishing criteria of bacterial and thermochemical sulfate

reduction," *Applied Geochemistry*, vol. 10, no. 4, pp. 373–389, 1995.

[99] H. G. Machel, "Bacterial and thermochemical sulfate reduction in diagenetic settings – old and new insights," *Sedimentary Geology*, vol. 140, no. 1-2, pp. 143–175, 2001.

[100] S. D. Yuan, I. M. Chou, and R. C. Burruss, "Disproportionation and thermochemical sulfate reduction reactions in S-H_2O-CH_4 and S-D_2O-CH_4 systems from 200 to 340 ˚C at elevated pressures," *Geochimica et Cosmochimica Acta*, vol. 118, pp. 263–275, 2013.

[101] R. Z. Hu, Y. Tao, H. Zhong, Z. L. Huang, and Z. W. Zhang, "Mineralisation systems of a mantle plume: a case study from the Emeishan igneous province, Southwest China," *Earth Science Frontiers*, vol. 12, no. 1, pp. 42–54, 2005.

[102] Z. L. Huang, J. Chen, and R. S. Han, *Geochemistry and Ore-Formation of the Huize Giant Lead–Zinc Deposit, Yunnan Province, China: Discussion on the Relationship between the Emeishan Flood Basalts and Lead–Zinc Mineralisation*, Geological Publishing House, Beijing, 2004.

[103] J. Wang, J. Zhang, W. B. Zhong, Q. Yang, F. K. Li, and Z. K. Zhu, "Sources of ore–forming fluids from Tianbaoshan and Huize Pb–Zn deposits in Yunnan–Sichuan–Guizhou region, Southwestern China: evidence from fluid inclusions and He–Ar isotopes," *Earth Science*, vol. 43, no. 6, pp. 2076–2099, 2018.

[104] Y. Xu, Z. Huang, D. Zhu, and T. Luo, "Origin of hydrothermal deposits related to the Emeishan magmatism," *Ore Geology Reviews*, vol. 63, pp. 1–8, 2014.

[105] A. Canals and E. Cardellach, "Ore lead and sulphur isotope pattern from the low-temperature veins of the Catalonian Coastal Ranges (NE Spain)," *Mineralium Deposita*, vol. 32, no. 3, pp. 243–249, 1997.

[106] M. L. Hou, X. Ding, and S. Y. Jiang, "Lead and sulfur isotope geochemistry of the Hexi gold deposit in Penglai, eastern Shandong," *Acta Geoscientica Sinica*, vol. 25, no. 2, pp. 145–150, 2004.

[107] S. Y. Jiang, T. Yang, L. Li, K. D. Zhao, and H. F. Ling, "Lead and sulfur isotopic compositions of sulfides from the TAG hydrothermal field, Mid-Atlantic Ridge," *Acta Petrologica Sinica*, vol. 22, no. 10, pp. 2597–2602, 2006.

[108] R. E. Zartman and B. R. Doe, "Plumbotectonics–the model," *Tectonophysics*, vol. 75, no. 1-2, pp. 135–162, 1981.

[109] C. X. Zhou, "The source of mineralizing metals, geochemical characterization of ore-forming solution, and metallogenetic mechanism of Qilinchang Zn–Pb deposit, Northeastern Yunnan Province, China," *Bulletin of Mineralogy, Petrology and Geochemistry*, vol. 17, no. 1, pp. 36–38, 1998.

[110] B. Li, *The Study of Fluid Inclusions Geochemistry and Tectonic Geochemistry of Lead–Zinc Deposits: Taking Huize and Songliang Lead–Zinc Deposits for Examples, in the Northeast of Yunnan Province, China*, Kunming University of Science and Technology, Kunming, 2010.

[111] L. M. Zhu, H. H. Yuan, and S. W. Luan, "A study of isotopic geochemical features and minerogenetic material source of the disu and Daliangzi Pb–Zn deposits, Sichuan," *Journal of Mineralogy and Petrology*, vol. 15, no. 1, pp. 72–79, 1995.

[112] M. Bao, J. X. Zhou, Z. L. Huang, and Z. G. Jin, "Dating methods for Pb–Zn deposits and chronology research progress of Sichuan–Yunnan–Guizhou Pb–Zn metallogenic province: a review," *Acta Mineralogica Sinica*, vol. 31, no. 3, pp. 391–396, 2011.

[113] J. X. Zhou, Z. L. Huang, G. F. Zhou, X. B. Li, W. Ding, and G. P. Bao, "Trace elements and rare earth elements of sulfide minerals in the tianqiao Pb–Zn ore deposit, Guizhou Province, China," *Acta Geologica Sinica-English Edition*, vol. 85, pp. 189–199, 2011.

[114] G. Faure, *Principles of Isotope Geology [M]*, John Wiley & Sons, New York, 1986.

[115] P. L. Cheng, W. Xiong, G. Zhou, and Z. W. He, "A preliminary study on the origins of ore-forming fluids and their migration directions for Pb–Zn deposits in NW Guizhou Province, China," *Acta Mineralogica Sinica*, vol. 35, no. 4, pp. 509–514, 2015.

[116] Z. W. Shen, C. H. Jin, Y. P. Dai, Y. Zhang, and H. Zhang, "Mineralisation age of the Maoping Pb-Zn deposit in the northeastern Yunnan Province: evidence from Rb–Sr isotopic dating of sphalerites," *Geological Journal of China Universities*, vol. 22, pp. 213–218, 2016.

[117] G. Faure, *Principles of Isotope Geology*, John Wiley & Sons, New York, 1977.

[118] F. H. Li and J. M. Qin, *Presinian System in Kangdian Area*, Chongqing Press, Chongqing, 1988.

[119] H. S. Chen and C. Y. Ran, *Geochemistry of Copper Deposit in Kangdian Area*, Geological Publishing House, Beijing, 1992.

[120] J. W. Mao, Z. H. Zhou, C. Y. Feng, Y. T. Wang, and C. Q. Zhang, "A preliminary study of the Triassic large-scale mineralisation in China and its geodynamic setting," *Geology China*, vol. 39, pp. 1437–1471, 2012.

[121] D. L. Leach, D. C. Bradley, D. Huston, S. A. Pisarevsky, R. D. Taylor, and S. J. Gardoll, "Sediment-hosted lead–zinc deposits in earth history," *Economic Geology*, vol. 105, pp. 593–625, 2010.

[122] K. Zaw, S. G. Peters, P. Cromie, C. Burrett, and Z. Hou, "Nature, diversity of deposit types and metallogenic relations of South China," *Ore Geology Reviews*, vol. 31, no. 1-4, pp. 3–47, 2007.

[123] D. L. Leach, D. Bradley, M. T. Lewchuk, D. T. Symons, G. de Marsily, and J. Brannon, "Mississippi valley-type lead–zinc deposits through geological time: implications from recent age-dating research," *Mineralium Deposita*, vol. 36, no. 8, pp. 711–740, 2001.